

Fort Hays State University  
**FHSU Scholars Repository**

---

Chemistry Faculty Publications

Chemistry

---

4-27-2003

## Effect of petrochemical industrial emissions of reactive alkenes and NO<sub>x</sub> on tropospheric ozone formation in Houston, Texas

T. B. Ryerson  
*National Oceanic and Atmospheric Administration*

M. Trainer  
*National Oceanic and Atmospheric Administration*

W. M. Angevine  
*National Oceanic and Atmospheric Administration*

C. A. Brock  
*National Oceanic and Atmospheric Administration*

R. W. Dissly  
*National Oceanic and Atmospheric Administration*

*See next page for additional authors*

Follow this and additional works at: [https://scholars.fhsu.edu/chemistry\\_facpubs](https://scholars.fhsu.edu/chemistry_facpubs)

 Part of the [Chemistry Commons](#)

---

### Recommended Citation

Ryerson, T. B., et al. (2003), Effect of petrochemical industrial emissions of reactive alkenes and NO<sub>x</sub> on tropospheric ozone formation in Houston, Texas, *J. Geophys. Res.*, 108, 4249, doi:10.1029/2002JD003070, D8.

This Article is brought to you for free and open access by the Chemistry at FHSU Scholars Repository. It has been accepted for inclusion in Chemistry Faculty Publications by an authorized administrator of FHSU Scholars Repository.

---

## Authors

T. B. Ryerson, M. Trainer, W. M. Angevine, C. A. Brock, R. W. Dissly, F. C. Fehsenfeld, G. J. Frost, P. D. Goldan, J. S. Holloway, G. Hübler, R. O. Jakoubek, W. C. Kuster, J. A. Neuman, D. K. Nicks, D. D. Parrish, J. M. Roberts, D. T. Sueper, E. L. Atlas, S. G. Donnelly, F. Flocke, A. Fried, W. T. Potter, S. Schauffler, V. Stroud, A. J. Weinheimer, B. P. Wert, C. Wiedinmyer, R. J. Alvarez, R. M. Banta, L. S. Darby, and C. J. Senff

## Effect of petrochemical industrial emissions of reactive alkenes and NO<sub>x</sub> on tropospheric ozone formation in Houston, Texas

T. B. Ryerson, M. Trainer, W. M. Angevine,<sup>1</sup> C. A. Brock,<sup>1</sup> R. W. Dissly,<sup>1,2</sup>  
F. C. Fehsenfeld,<sup>1</sup> G. J. Frost,<sup>1</sup> P. D. Goldan, J. S. Holloway,<sup>1</sup> G. Hübler,<sup>1</sup>  
R. O. Jakoubek, W. C. Kuster, J. A. Neuman,<sup>1</sup> D. K. Nicks Jr.,<sup>1</sup> D. D. Parrish,  
J. M. Roberts, and D. T. Sueper<sup>1</sup>

Aeronomy Laboratory, National Oceanic and Atmospheric Administration, Boulder, Colorado, USA

E. L. Atlas, S. G. Donnelly, F. Flocke, A. Fried, W. T. Potter, S. Schauffler, V. Stroud,  
A. J. Weinheimer, B. P. Wert, and C. Wiedinmyer

Atmospheric Chemistry Division, National Center for Atmospheric Research, Boulder, Colorado, USA

R. J. Alvarez,<sup>1</sup> R. M. Banta, L. S. Darby,<sup>1</sup> and C. J. Senff<sup>1</sup>

Environmental Technology Laboratory, National Oceanic and Atmospheric Administration, Boulder, Colorado, USA

Received 23 October 2002; revised 8 January 2003; accepted 9 January 2003; published 25 April 2003.

[1] Petrochemical industrial facilities can emit large amounts of highly reactive hydrocarbons and NO<sub>x</sub> to the atmosphere; in the summertime, such colocated emissions are shown to consistently result in rapid and efficient ozone (O<sub>3</sub>) formation downwind. Airborne measurements show initial hydrocarbon reactivity in petrochemical source plumes in the Houston, TX, metropolitan area is primarily due to routine emissions of the alkenes propene and ethene. Reported emissions of these highly reactive compounds are substantially lower than emissions inferred from measurements in the plumes from these sources. Net O<sub>3</sub> formation rates and yields per NO<sub>x</sub> molecule oxidized in these petrochemical industrial source plumes are substantially higher than rates and yields observed in urban or rural power plant plumes. These observations suggest that reductions in reactive alkene emissions from petrochemical industrial sources are required to effectively address the most extreme O<sub>3</sub> exceedences in the Houston metropolitan area.

*INDEX TERMS:* 0345 Atmospheric Composition and Structure: Pollution—urban and regional (0305); 0365 Atmospheric Composition and Structure: Troposphere—composition and chemistry; 0368 Atmospheric Composition and Structure: Troposphere—constituent transport and chemistry; *KEYWORDS:* Houston ozone formation, petrochemical alkene emissions

**Citation:** Ryerson, T. B., et al., Effect of petrochemical industrial emissions of reactive alkenes and NO<sub>x</sub> on tropospheric ozone formation in Houston, Texas, *J. Geophys. Res.*, 108(D8), 4249, doi:10.1029/2002JD003070, 2003.

### 1. Introduction

[2] Ozone (O<sub>3</sub>) is formed in the troposphere by photochemical reactions involving the oxides of nitrogen NO and NO<sub>2</sub> (summed as NO<sub>x</sub>) and reactive volatile organic compounds (VOCs) [Crutzen, 1979; Haagen-Smit, 1952; Leighton, 1961; Levy, 1971]. Model studies have shown that O<sub>3</sub> formation rates and yields are dependent upon both the absolute concentrations of NO<sub>x</sub> and VOCs and upon the ratios of these species [e.g., Derwent and Davies, 1994; Liu et al., 1987; Sillman, 2000]. Results from ambient measurements have confirmed that substantial differences in the rate

and magnitude of O<sub>3</sub> production consistently occur in plumes downwind of different anthropogenic source types, characterized by different NO<sub>x</sub> and VOC emissions rates and the VOC/NO<sub>x</sub> ratios that result [e.g., Daum et al., 2000a; Gillani et al., 1998; Luria et al., 2000; Neuman et al., 2002; Nunnermacker et al., 2000; Ryerson et al., 1998, 2001].

[3] Three anthropogenic source types with contrasting emissions rates and VOC/NO<sub>x</sub> ratios are fossil-fueled electric power plants, the transportation sources typical of urban areas, and the petrochemical industry. The first two combined account for approximately 75% of total U.S. anthropogenic NO<sub>x</sub> emissions annually [EPA, 2001]. Fossil-fueled electric power plants are very concentrated point sources of NO<sub>x</sub> but do not emit appreciable amounts of VOCs. Thus O<sub>3</sub> production observed in plumes downwind of isolated, rural power plants in the U.S. [e.g., Davis et al., 1974] occurs as a result of mixing plume NO<sub>x</sub> with primarily

<sup>1</sup>Also at Cooperative Institute for Research in Environmental Sciences, University of Colorado, Boulder, Colorado, USA.

<sup>2</sup>Now at Ball Aerospace Corporation, Boulder, Colorado, USA.

biogenic reactive VOCs, especially with isoprene [Chameides *et al.*, 1988; Trainer *et al.*, 1987a, 1987b], over time during plume transport. Measurements confirm the strong dependence of O<sub>3</sub> production on NO<sub>x</sub> concentration [Gillani *et al.*, 1998; Nunnermacker *et al.*, 2000; Ryerson *et al.*, 1998] and on ambient VOC concentration and reactivity [Luria *et al.*, 2000; Ryerson *et al.*, 2001].

[4] Power plant plume VOC/NO<sub>x</sub> ratios can be sufficiently low that O<sub>3</sub> formation is initially suppressed in favor of efficient nitric acid (HNO<sub>3</sub>) production, removing NO<sub>x</sub> from further participation in O<sub>3</sub> formation cycles [Neuman *et al.*, 2002; Ryerson *et al.*, 2001]. In contrast, the tailpipe emissions that dominate urban areas are sources of both NO<sub>x</sub> and VOCs. The many small individual sources contributing to urban emissions are usually considered together as an area source dispersed over tens to hundreds of square kilometers. As a result, urban plumes are relatively dilute, with total NO<sub>x</sub> emissions rates comparable to those from power plants but dispersed over a much larger area. Coemission in this manner results in initial VOC/NO<sub>x</sub> ratios that favor O<sub>3</sub> formation immediately upon emission, typically leading to faster O<sub>3</sub> production rates and higher yields in urban plumes than in concentrated power plant plumes [Daum *et al.*, 2000a; Luria *et al.*, 1999; Nunnermacker *et al.*, 2000].

[5] The fastest rates of O<sub>3</sub> formation, and the highest yields per NO<sub>x</sub> molecule emitted, are predicted for conditions where strongly elevated concentrations of NO<sub>x</sub> and reactive VOCs are simultaneously present. These conditions can be routinely found in the NO<sub>x</sub>- and VOC-rich plumes from petrochemical industrial facilities [e.g., Sexton and Westberg, 1983]. Petrochemical NO<sub>x</sub> emissions are a by-product of fossil-fuel combustion for electric power generation, for heat generation, and from flaring of unwanted volatile materials; NO<sub>x</sub> emission from a large petrochemical facility can approach that from a large electric utility power plant. While a given facility may have hundreds of combustion sources, spread over many square kilometers, the majority of petrochemical NO<sub>x</sub> emissions typically come from only a few of the largest sources. Thus concentrations of NO<sub>x</sub> in plumes from large petrochemical facilities are typically much higher than in those from urban areas. Sources of VOC emissions from a petrochemical industrial facility are thought to be much more numerous than sources of NO<sub>x</sub>. VOCs can be emitted via continuous emissions from stacks, episodic emissions specific to individual processes, and leaks from pipes and valving. The wide variety of VOC compounds typically emitted from petrochemical facilities, with differing reactivities toward the hydroxyl radical (OH), must be considered to understand the O<sub>3</sub>-forming potential of these sources [Carter, 1994; Derwent, 2000; Watson *et al.*, 2001].

[6] The greater Houston, TX, metropolitan area is distinguished by the largest concentration of petrochemical industrial facilities in the U.S. (Figure 1). Further, Houston is noted for some of the highest O<sub>3</sub> mixing ratios routinely encountered in the continental U.S. in the present-day. As a result, photochemical O<sub>3</sub> and aerosol production in the Houston area was the focus of the Texas Air Quality Study 2000 field project [Brock *et al.*, 2003; Kleinman *et al.*, 2002; Neuman *et al.*, 2002; Wert *et al.*, 2003]. We report measurements taken from an instrumented aircraft during

that project to evaluate the effects of petrochemical industrial emissions on tropospheric O<sub>3</sub> formation. First, we analyze O<sub>3</sub> production in spatially resolved plumes from the geographically isolated complexes at Sweeny, Freeport, and Chocolate Bayou (Figure 1). We then extend this analysis to include data from coalesced plumes downwind of multiple petrochemical complexes in the heavily industrialized Houston Ship Channel and Texas City areas. Finally, O<sub>3</sub> production in petrochemical industrial plumes is compared to that observed downwind of urban areas and rural, fossil-fueled electric utility power plants.

## 2. Experimental Procedure

[7] The National Center for Atmospheric Research L-188C Electra aircraft leased by the National Oceanic and Atmospheric Administration (NOAA) was based at Ellington Field, Houston, TX, as part of the Texas Air Quality Study in August and September 2000. Instrumentation aboard the Electra included 1-Hz measurements of O<sub>3</sub>, nitric oxide (NO), nitrogen dioxide (NO<sub>2</sub>), HNO<sub>3</sub>, total reactive nitrogen (NO<sub>y</sub>), carbon monoxide (CO), carbon dioxide (CO<sub>2</sub>), sulfur dioxide (SO<sub>2</sub>), and spectrally resolved actinic flux [Holloway *et al.*, 2000; Neuman *et al.*, 2002; Nicks *et al.*, 2003; Ryerson *et al.*, 1998, 1999, 2000]. Formaldehyde (CH<sub>2</sub>O) was measured by tunable diode laser absorption spectrometry [Fried *et al.*, 1998; Wert *et al.*, 2003] at 10-s resolution for 27 and 28 August, the two flights reported here. Peroxyacyl nitrate compounds (e.g., peroxyacetyl nitrate (PAN)) were measured once every 3.5 min by gas chromatography (GC) using electron capture detection. GC measurements, either performed in situ [Goldan *et al.*, 2000] or as a whole-air sample (WAS) from canisters [Schauffler *et al.*, 1999], provided speciated data on an extensive set of VOCs (Table 1). Thirty-nine WAS canisters were sampled on each flight; in addition to the VOCs, the WAS instrument provided data on CO, methane (CH<sub>4</sub>), C<sub>1</sub> through C<sub>5</sub> monofunctional alkyl nitrate compounds (RONO<sub>2</sub>), and a variety of other halogenated species.

### 2.1. Measurement Uncertainties

[8] Here we briefly assess uncertainties in the chemical measurements most relevant to the following analyses. Calibrations of the reactive nitrogen (NO, NO<sub>2</sub>, HNO<sub>3</sub>, PAN compounds, and total NO<sub>y</sub>) measurements are conservatively estimated to be accurate to better than ±10% based on in-flight standard addition calibration data, multiple internal consistency checks, and extensive intercomparison with other aircraft and ground measurements of these species [Neuman *et al.*, 2002]. In addition to uncertainties in calibration, estimated imprecision for the 1 Hz reactive nitrogen measurements at low mixing ratios varied between ±20 parts per trillion by volume (pptv) for NO to ±150 pptv for NO<sub>y</sub>. Both the NO<sub>y</sub> chemiluminescence instrument and the HNO<sub>3</sub> chemical ionization mass spectrometer have been shown to sample atmospheric HNO<sub>3</sub> rapidly and quantitatively during flight [Neuman *et al.*, 2002; Ryerson *et al.*, 2000]. Tight correlation ( $r^2 = 0.962$ ), a linear least squares fitted slope of  $0.96 \pm 0.05$ , and an intercept of 22 pptv suggests that no systematic bias existed between the sum of (NO + NO<sub>2</sub> + HNO<sub>3</sub> + PAN) compounds and the total NO<sub>y</sub>.

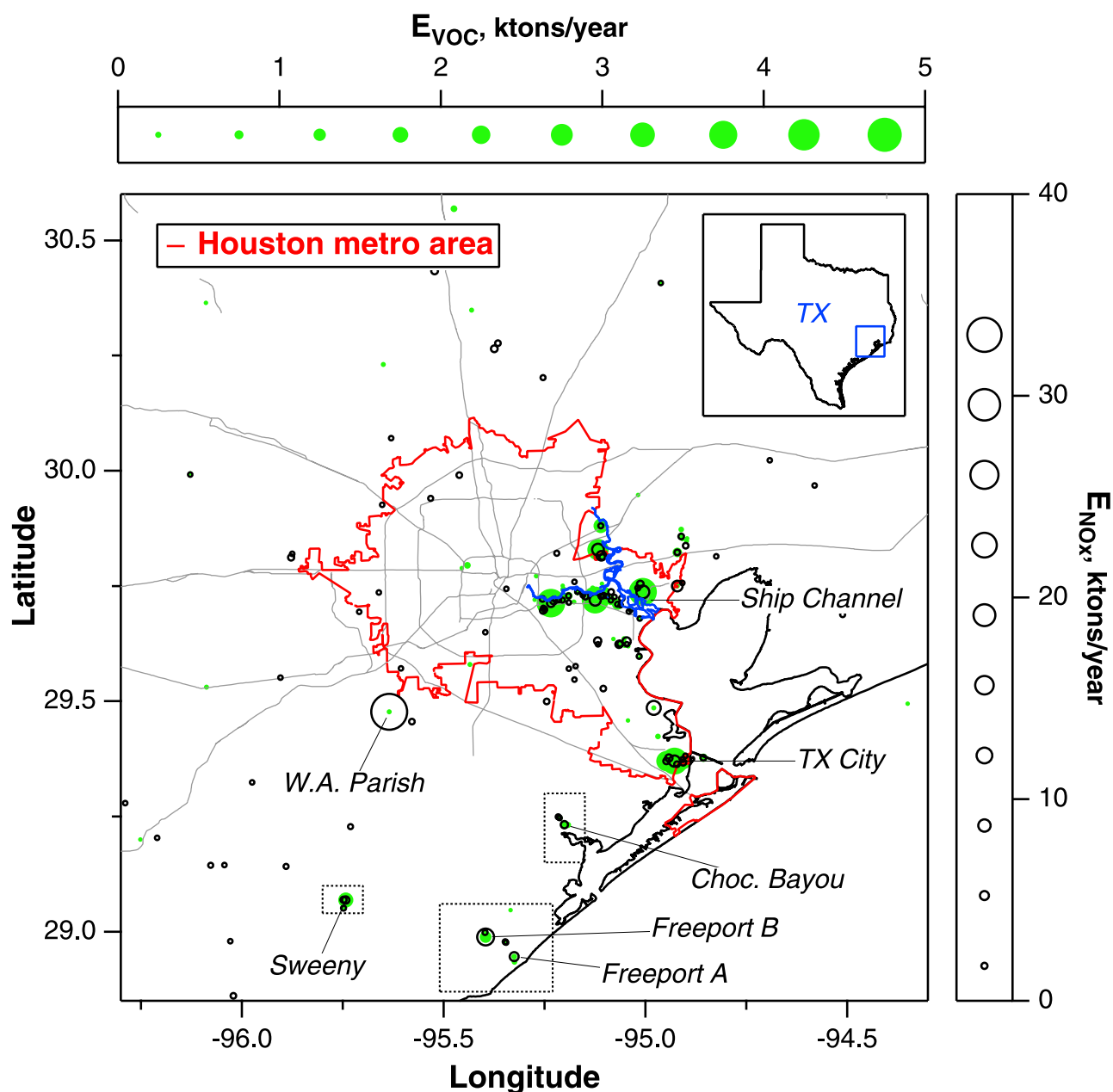


**Figure 1.** A  $200 \times 200$  km map centered on the greater Houston metropolitan area (red line), showing the study region for Electra research flights of 27 and 28 August 2000. Locations of point emission sources are shown sized according to volatile organic compound emission source strengths (“ $E_{\text{VOC}}$ ,” filled green circles) and  $\text{NO}_x$  emission source strengths (“ $E_{\text{NO}_x}$ ,” open black circles) according to the legends provided. Emissions data are taken from the 2000 Texas Natural Resource Conservation Commission point source database; only sources greater than 100 t/yr are shown. The Houston Ship Channel is east of the Houston urban center, surrounded by numerous petrochemical facilities at  $29.7^\circ$  latitude; other major petrochemical complexes and power plants are labeled.

measurement over the course of the field mission [e.g., Neuman *et al.*, 2002]. The fractional contribution of  $\text{C}_1\text{-C}_5$   $\text{RONO}_2$  compounds (measured in the WAS) ranged between 0.01 and 0.02 of total  $\text{NO}_y$ , similar to or slightly lower than previous studies [Bertman *et al.*, 1995; Flocke *et al.*, 1991; Ridley *et al.*, 1997]. Although coincident alkyl nitrate and PAN data are very sparse, inclusion of the average  $\text{RONO}_2$  fraction of 0.015 in the above  $\text{NO}_y$  budget brings the sum very close to 1, indicating that all the major

components of the reactive nitrogen family were measured accurately.

[9] Comparison of the two independent CO measurements aboard the Electra (GC analysis of WAS canisters [Schaufler *et al.*, 1999] and vacuum-ultraviolet resonance fluorescence [Holloway *et al.*, 2000]) showed tight correlation ( $r^2 = 0.989$ ), a fitted linear least squares slope of 1.03, and an intercept of 4 parts per billion by volume (ppbv), suggesting that both instruments measured ambient CO to

**Table 1.** Names and OH Rate Coefficients ( $k_{\text{OH}}$ ) for Hydrocarbon Compounds and Selected Other Species Measured Aboard the Electra Used in This Report<sup>a</sup>

Alkanes	$k_{\text{OH}}$	Alkenes	$k_{\text{OH}}$	Aromatics	$k_{\text{OH}}$	Alkynes	$k_{\text{OH}}$	Others	$k_{\text{OH}}$
<b>Ethane</b>	0.3	<b>ethene</b>	9	<b>benzene</b>	1.2	<b>ethyne</b>	0.9	CO	0.2
<b>Propane</b>	1.1	<b>propene</b>	26	<b>methylbenzene (toluene)</b>	6.0	propyne	5.9	CH <sub>4</sub>	0.007
<b><i>n</i>-Butane</b>	2.4	<b>1-butene</b>	31	ethylbenzene	7.1			CH <sub>3</sub> CHO	17
<b>2-Methylpropane</b>	2.2	<b><i>cis</i>-2-butene</b>	56	1,2-dimethylbenzene	13.7			CH <sub>2</sub> O	8
<b><i>n</i>-Pentane</b>	4.0	<b><i>trans</i>-2-butene</b>	64	1,3- and 1,4-dimethylbenzene	20			NO <sub>2</sub>	9
2-Methylbutane	3.7	1,3-butadiene	67	phenylethene (styrene)	58				
Cyclopentane	5.0	1-pentene	31	2-methylethylbenzene	12.3				
<i>n</i> -Hexane	5.5	2-methyl-2-butene	87	<i>n</i> -propylbenzene	6.0				
2-Methylpentane	5.3	3-methyl-1-butene	32	1,3,5-trimethylbenzene	58				
2,2-Dimethylbutane	2.3	<i>trans</i> -2-pentene	67	1,2,4-trimethylbenzene	33				
2,3-Dimethylbutane	6.0	<i>cis</i> -2-pentene	65	1,2,3-trimethylbenzene	33				
3-Methylpentane	5.4	cyclopentene	67						
Methylcyclopentane	5.7	<b>2-methyl-1,3-butadiene (isoprene)</b>	101						
<b>Cyclohexane</b>	7.2								
<b><i>n</i>-Heptane</b>	7.0								
<b>2-Methylhexane</b>	7.0								
3-Methylhexane	7.5								
2,3-Dimethylpentane	7.1								
2,4-Dimethylpentane	5.0								
Methylcyclohexane	10.0								
<b><i>n</i>-Octane</b>	8.7								
<b>2,2,4-Trimethylpentane</b>	3.6								
<i>cis</i> - and <i>trans</i> -1,3-Dimethylcyclohexane	9.5								
<i>n</i> -Nonane	10.0								
<i>n</i> -Decane	11.2								

<sup>a</sup>Normal type indicates compounds measured only in the whole-air canister samples, italicized type indicates those measured only in the in situ GC, and bold type indicates those measured in both systems. Rate coefficients ( $k_{\text{OH}}$ , in units of  $10^{-12}$  cm<sup>3</sup> molec/s) calculated for 298 K and 1013 mb from data in the work of Atkinson [1994, 1997] and DeMore *et al.* [1997]. CO, CH<sub>4</sub>, NO<sub>2</sub>, CH<sub>2</sub>O, and CH<sub>3</sub>CHO are included for comparison.

within the stated uncertainties of the two techniques [Nicks *et al.*, 2003]. The CH<sub>2</sub>O measurement has been critically evaluated to characterize its time response, precision, and accuracy, and the data were compared to a ground-based long-path measurement using differential optical absorption spectroscopy (DOAS) [Stutz and Platt, 1997]. These tests suggest the 10-s CH<sub>2</sub>O data onboard the Electra are accurate to better than  $\pm(120 \text{ pptv} + 10\%)$  [Wert *et al.*, 2003]. The 1-s O<sub>3</sub> measurement by NO-induced chemiluminescence was compared to a UV-absorption measurement aboard the Electra, and to a separate UV-absorption measurement during overflights of an instrumented ground site, and shown to be accurate within the stated uncertainty of  $\pm(0.3 \text{ ppbv} + 3\%)$ . VOC data were compared between the WAS measurements and the in situ GC and found to be accurate, within stated experimental uncertainties of  $\pm 10\%$  or less, for the compounds reported here at the elevated mixing ratios relevant to this report. Generally, the uncertainty of the SO<sub>2</sub> measurement was within  $\pm 10\%$  for SO<sub>2</sub> levels well above the detection limit of approximately 0.5 ppbv. However, for the data on the two flights presented here, this accuracy was sporadically degraded by short-term transients, of up to several parts per billion by volume, due to operational difficulties with the in-flight calibration system. The SO<sub>2</sub> data are used here only in a relative sense, e.g., to distinguish between different anthropogenic source types by noting the presence or absence of elevated SO<sub>2</sub> in a given plume.

## 2.2. Meteorological and Emissions Data

[10] Information on wind speed and direction, mixed layer heights, and vertical mixing within and above the

mixed layer is derived from on-board chemical and meteorological measurements [Ryerson *et al.*, 1998] and observations from other airborne [Senff *et al.*, 1998] and ground-based [Angevine *et al.*, 1994] remote-sensing instrumentation deployed throughout the area for the Texas 2000 study. Uncertainties in wind speeds of  $\pm 1$  m/s and in boundary layer heights of  $\pm 10\%$  are estimated by comparing derived values from the various aircraft- and ground-based data sets. Tabulated information on source emissions was obtained from and, where possible, crosschecked between various inventory databases. These included the U.S. Environmental Protection Agency (EPA) AIRS, TRI, and E-Grid databases ([www.epa.gov/ttn/chief](http://www.epa.gov/ttn/chief)), as well as from information provided by plant operators to the Texas Natural Resource Conservation Commission (TNRCC) for the 2000 reporting year ([www.tnrcc.state.tx.us/air/aqp/psei.html](http://www.tnrcc.state.tx.us/air/aqp/psei.html)). We use the TNRCC point source database (PSDB) for 2000 as the primary reference in this report. Hourly averaged emissions data, from continuous emission monitoring systems (CEMS) and from estimates provided by facility operators, were also examined for the time periods of the present study. The timing and nature of nonroutine-emission events, or upsets, at many facilities was also reported to TNRCC and are taken into account in the present analysis.

## 2.3. Plume Identification

[11] Plumes from different sources are distinguished by markedly different enhancements above background of many of the chemical species measured aboard the Electra aircraft, reflecting the different emissions profiles from each source type. Fossil-fueled electric utility power plant plumes show relatively strong enhancements in NO<sub>y</sub> species



and CO<sub>2</sub>. SO<sub>2</sub> can also be strongly enhanced in power plant plumes if sulfur-rich fuels are used and emissions are not treated to remove it; typically, coal- and oil-fired units emit substantial amounts of SO<sub>2</sub>, while natural-gas-fired turbine units do not. CO enhancements are typically negligible in power plant plumes, with some exceptions [Nicks *et al.*, 2003]. Substantial VOC enhancements in power plant plumes are never detected. Urban plumes are characterized by substantial enhancements in CO and VOCs, typical of tailpipe combustion sources [Harley *et al.*, 2001]; NO<sub>y</sub> species and CO<sub>2</sub> are also enhanced but to a lesser degree than in power plant plumes. SO<sub>2</sub> is not typically substantially enhanced in urban plumes. Plumes from petrochemical complexes have varied chemical composition, but typically have enhanced NO<sub>x</sub> and CO<sub>2</sub> characteristic of the embedded power plants required to supply electricity and heat to the facilities. Petrochemical plumes can also be characterized by elevated CO levels and elevated SO<sub>2</sub> depending on the fuel source. Enhanced VOC levels specific to individual processes and facilities are also characteristic of petrochemical source plumes [Watson *et al.*, 2001]. Thus examination of the chemical data in conjunction with aircraft position, wind speed, and wind direction information permits identification of plumes from different sources until they are nearly fully mixed with each other or with background air.

[12] Plume chemical and dynamic evolution was tracked from the Electra aircraft by performing crosswind transects within the mixed layer at successive distances downwind of individual sources and source complexes [e.g., Brock *et al.*, 2003; Ryerson *et al.*, 1998]. These data were taken between noon and 1700 hours local standard time, at times of day when mixing was most rapid, so that compounds emitted from a source were rapidly and extensively mixed within the boundary layer. Emissions from an individual petrochemical complex are treated as coming from a single or at most a few point emitters for transects performed >10 km or a few source diameters downwind [Wert *et al.*, 2003]. This is justified by downwind observations of multiple Ship Channel point source plumes on these two flight days; originally separated plumes became mutually indistinguishable between successive afternoon transects 15 km apart, or roughly an hour of transport time downwind.

### 3. Results

[13] Hourly averaged O<sub>3</sub> mixing ratios measured at surface sites can exceed 200 ppbv during severe summertime pollution episodes in the Houston metropolitan area. Previous studies in Houston have suggested these extreme O<sub>3</sub> exceedences are more common on days characterized by relatively complex meteorological conditions and can be frequent during stagnation episodes [Davis *et al.*, 1998]. For Sunday, 27 August, and Monday, 28 August 2000, however, no exceedence of the 1 hour, 120 ppbv Federal air quality standard was recorded in the Houston metropolitan area, in part due to steady ventilation by relatively clean southerly winds from the Gulf of Mexico. Despite relatively low O<sub>3</sub> mixing ratio enhancements, Electra research flights on these 2 days provided data from which O<sub>3</sub> formation rates and yields downwind of different anthropogenic source types are determined under relatively uniform-flow conditions.

We analyze data from these days specifically because the prevailing wind direction provided spatially separated and relatively well-resolved plumes from several isolated petrochemical industrial facilities, the W.A. Parish power plant, the multiple petrochemical complexes along the Ship Channel, and the urban core of Houston itself.

[14] We present data on photochemical O<sub>3</sub> production from emissions released during the morning and early afternoon hours and observed within 15 min to ca. 8 hours following release. These findings are most relevant to typical Houston summertime conditions characterized by low to moderate background O<sub>3</sub> levels (40–60 ppbv) coupled with substantial and rapid O<sub>3</sub> production (within 4 hours of release) in a single day. This characteristic is unique to Houston and is in contrast to other urban areas in the U.S., in which the highest O<sub>3</sub> mixing ratios typically result from slower accumulation of O<sub>3</sub> over the period of several days [e.g., Banta *et al.*, 1998; Daum *et al.*, 2000b; Kleinman *et al.*, 2000; Winner and Cass, 1999].

#### 3.1. Isolated Petrochemical Industrial Complexes

[15] Aircraft flights on 27 and 28 August 2000 sampled the spatially resolved plumes from several isolated petrochemical complexes south of the Houston metropolitan area (Figure 2). These plumes were composed of the aggregated emissions from groupings of chemical plants in well-segregated areas several kilometers in extent. On both days, emissions plumes from complexes at Sweeny, Freeport, and Chocolate Bayou were carried inland by steady winds at  $4.5 \pm 1.0$  m/s at  $160^\circ \pm 16^\circ$  from the Gulf of Mexico. Measurements upwind over the Gulf on both days characterized the inflow as relatively clean, devoid of appreciable amounts of reactive VOCs or NO<sub>x</sub>, with CO levels below 100 ppbv and O<sub>3</sub> roughly 35 ppbv. For the isolated sources, we establish that the source of enhanced plume levels of NO<sub>x</sub> and VOCs, and the O<sub>3</sub> and other photoproduct formation, are due to emissions from the petrochemical facilities themselves. The plume transect data are then used to estimate VOC/NO<sub>x</sub> emissions ratios, NO<sub>x</sub> oxidation rates, HNO<sub>3</sub> production rates, net O<sub>3</sub> production rates and yields, and to determine the primary species contributing to OH reactivity in these petrochemical emissions plumes.

##### 3.1.1. Emissions Sources

[16] Enhancements of NO<sub>x</sub>, CO, CO<sub>2</sub>, and VOCs, and secondary photoproducts including O<sub>3</sub>, CH<sub>2</sub>O, CH<sub>3</sub>CHO, and PAN compounds, observed in these isolated plumes can be unambiguously attributed to emissions from the petrochemical facilities at each location. Potential emissions of NO<sub>x</sub> and reactive hydrocarbons from colocated automobile, truck, ship, and rail traffic in the area are ruled out as significant contributors to the totals emitted from these three complexes. The fraction of on-road transportation, or tailpipe, emissions from automobiles and trucks is expected to have been minimal owing to the location of these complexes, which are remote from city or town centers and are characterized by low roadway densities in all three source areas (Figure 1). Recent reports suggest that such tailpipe emissions result in tightly correlated enhancements in CO and NO<sub>x</sub>, with characteristic morning emissions ratios in 2000 of roughly 5–6 (mol CO/mol NO<sub>x</sub>) [Harley *et al.*, 2001; Parrish *et al.*, 2002]. These values are in good agreement with tailpipe CO/NO<sub>x</sub> emissions ratios of  $6 \pm 1$ ,

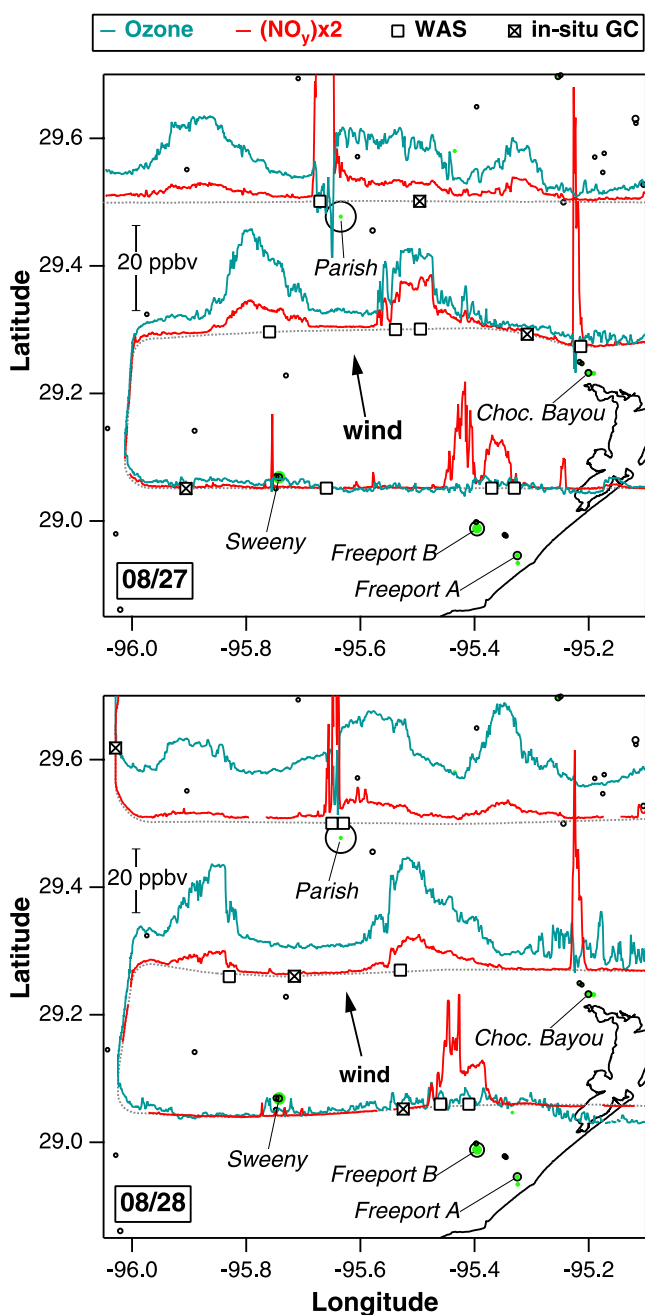


**Figure 2.** A  $90 \times 90$  km detail view of the map shown in Figure 1, showing measured ozone and  $\text{NO}_y$  values plotted relative to aircraft position along the SW portions of the flight tracks on 27 August (first panel) and 28 August (second panel). Symbols along the flight tracks give sample locations for the whole-air canisters (WAS, open squares) and in situ gas chromatography (barred squares). Winds on both days were steady from  $160^\circ$  at 4.5 m/s. The scale bars show a 20 ppbv equivalent enhancement in ozone.

estimated from Electra data taken in late-morning transects of the Houston urban core. In contrast, for transects flown very close to the isolated petrochemical facilities, observed enhancements of these species were often poorly correlated, suggesting physically separate emissions of CO and  $\text{NO}_x$  uncharacteristic of tailpipe sources. CO/ $\text{NO}_x$  ratios meas-

ured in plume transects within 10 km of the three isolated petrochemical complexes varied, ranging from 0.1 to nearly 1, further illustrating that the  $\text{NO}_x$  was not emitted from tailpipe sources.

[17] Ratios of hydrocarbons to ethyne (acetylene;  $\text{C}_2\text{H}_2$ ) measured in plume transects also rule out tailpipe sources as substantial contributors to the observed enhancements in the isolated petrochemical facility plumes. Tailpipe emissions have characteristic ratios of (ethene ( $\text{C}_2\text{H}_4$ )/ethyne) ranging from 1 to 3 and (propene ( $\text{C}_3\text{H}_6$ )/ethyne) from 0.5 to 1.5, determined from airborne VOC measurements above the urban cores of Nashville, TN, and Atlanta, GA, in 1999, and in Houston and Dallas, TX, in 2000. Atmospheric oxidation processes decrease these two ratios over time between emission and measurement, primarily due to the substantially faster OH reaction rate coefficients of  $\text{C}_2\text{H}_4$  and  $\text{C}_3\text{H}_6$  compared to ethyne (Table 1). Nonetheless, the ratios in the urban plumes observed from aircraft are in good agreement with recent tunnel measurements in both Houston (W. Lonneman, unpublished data, 2000) and in Nashville [Harley *et al.*, 2001]. In contrast, observed molar ratios in near-field transects of the plumes from a variety of petrochemical facilities in the Houston study region for ( $\text{C}_2\text{H}_4$ /ethyne) ranged from 10 to 30 and for ( $\text{C}_3\text{H}_6$ /ethyne) from 5 to 40. These values are substantially higher than ratios from tailpipe sources, confirming that the contribution of alkenes from tailpipe sources was negligible in these plumes.

[18] For the isolated facilities, the absence of substantially elevated  $\text{SO}_2$  in these plumes is characteristic of gas-fired turbine exhaust and suggests that locomotive and marine diesel emissions, which are typically rich in  $\text{SO}_2$  [Corbett and Fischbeck, 1997], are not significant sources of  $\text{NO}_x$  in the plumes studied here. Small enhancements of  $\text{SO}_2$  observed in the Freeport plume are qualitatively consistent with emissions from the Gulf Chemical and Metallurgical Plant, a known  $\text{SO}_2$  source within the Freeport complex [Brock *et al.*, 2003]. We conclude the observed plume enhancements are due to emissions of reactive VOC and  $\text{NO}_x$  directly from the petrochemical facilities themselves.

[19] While other colocated sources are ruled out as substantial contributors to the isolated petrochemical plumes, these plumes may have entrained emissions from other sources during transport. For example, the wind direction on the 2 days considered here advected the Sweeny plume over a wooded area to the north-northwest, which is a known weak biogenic source of isoprene [Wiedinmyer *et al.*, 2001]. This acted to continually replenish the Sweeny plume with low but nonnegligible amounts of isoprene during transport. Plumes from the petrochemical complexes south of Houston, as well as that from the W.A. Parish power plant, eventually were transported over the western and southern edges of the Houston urban area, with additional mixing of urban tailpipe emissions into the aged plumes. The overall impact of entrainment during transport on derived  $\text{NO}_x$  oxidation rates, and plume production rates of  $\text{O}_3$  and other secondary products, is shown below to be relatively minor.

### 3.1.2. VOC Reactivity

[20] WAS canisters taken in resolved plumes from the three isolated petrochemical complexes show elevated mixing ratios of many of the measured hydrocarbons (Table 1), including substantial enhancements in alkanes, alkenes,



aromatics, and ethyne. In general, the compounds ethane ( $C_2H_6$ ),  $C_2H_4$ , propane ( $C_3H_8$ ),  $C_3H_6$ , and isomers of butane and pentane were the most abundant, with differing relative abundances characteristic of the three source complexes. However, the contribution of an individual hydrocarbon species to prompt  $O_3$  formation is determined both by its concentration and by how rapidly that compound can react with OH, which is the rate limiting step in  $O_3$  formation [e.g., Atkinson, 1994, 1997; DeMore *et al.*, 1997]. Alkenes and larger aromatic compounds typically have relatively large OH rate coefficients (Table 1); thus these compounds will contribute more to prompt  $O_3$  production at a given concentration than will alkanes or alkynes. To elucidate the directly emitted VOCs primarily responsible for plume  $O_3$  formation, the hydrocarbon data are presented in Figure 3 by multiplying the concentration of each measured species by the appropriate OH rate coefficient at the measured ambient temperature and pressure. The black horizontal bars in Figures 3a and 3c show total OH reactivity calculated from the measured VOCs, excluding the photoproducts  $CH_2O$  and acetaldehyde ( $CH_3CHO$ ). While plume OH reactivities due to  $NO_2$ ,  $CH_4$ , and CO are not negligible (Figures 3a and 3c), the large increases over reactivities calculated from samples taken outside the plumes are almost entirely due to petrochemical VOC emissions. Further examination of the individually speciated VOC data shows that of the many compounds emitted and measured, two compounds alone account for the majority of the plume reactivity above the background. The data in Figures 3b and 3d from both days show that the principal reaction partners for OH in all three plumes were the directly emitted alkenes  $C_2H_4$  and  $C_3H_6$  and their oxidation products. Mixing ratios of  $C_2H_4$  and  $C_3H_6$  observed within 5 km of these sources exceeded background levels by factors ranging from 20 to over 200. Elevated plume levels of the reactive alkenes  $C_2H_4$  and  $C_3H_6$  and their photooxidation products  $CH_2O$  and  $CH_3CHO$  are sufficient to dominate OH reactivity for some time after emission. For example, in the  $\sim 20$ -min-old Chocolate Bayou plume sampled at 1902 UT (1302 hours local time) on 27 August (Figure 3a),  $C_2H_4$  and  $C_3H_6$  account for  $>80\%$  of the OH reactivity calculated from the measured hydrocarbons (Table 1). Even in the  $\sim 45$ -min-old Freeport plume,  $C_2H_4$  and  $C_3H_6$  still account for 75% of OH reactivity.

[21] As these alkenes are rapidly consumed, their photo-products  $CH_2O$  and  $CH_3CHO$  increase in relative importance as OH partners, acting to further propagate the radical chain leading to  $O_3$  formation. Measurements of plume  $CH_2O$  show that direct emissions of this compound are negligibly small compared to  $CH_2O$  formed during transport from the OH-induced oxidation of the directly emitted VOCs, primarily  $C_2H_4$  and  $C_3H_6$  [Wert *et al.*, 2003]. The  $CH_2O$  derived from alkene oxidation, once formed, constitutes a major reaction partner for OH in all these plumes, and photolysis of  $CH_2O$  becomes an important free radical source.  $CH_2O$  and  $CH_3CHO$  are themselves relatively short-lived, and within hours the longer-lived alkane compounds are observed to dominate plume reactivity downwind. However, by then, the shorter-lived  $NO_x$  had already been extensively oxidized.

[22] The presence of elevated mixing ratios of longer-lived alkanes suggests that  $O_3$  formation may have con-

tinued beyond the final aircraft transect downwind ( $\sim 60$  km), catalyzed by the remaining  $NO_x$ , additional  $NO_x$  from other downwind sources, and that recycled from thermal decomposition of PAN-type compounds. However, the remaining alkanes will oxidize relatively slowly thereafter, and alkane reaction products are predominantly the less-reactive ketones [Atkinson, 1997]. Given the low observed mixing ratios of  $NO_x$  and reactive VOC remaining at these distances, and the observed decrease in  $O_3$  production rates between successive transects, the rate at which  $O_3$  would be formed is also expected to be substantially lower downwind. The evolution over time of plume  $CH_2O$  mixing ratios [Wert *et al.*, 2003] further suggests that reservoirs of compounds serving as precursors to peroxy radical formation in the plumes were also relatively depleted at these distances. Thus  $O_3$  formation downwind of the final Electra transects (plume ages  $>4$  hours) in the isolated petrochemical plumes is expected to have been relatively minor compared to that observed on the timescales considered here. The majority of  $O_3$  produced in these plumes is therefore ascribed to colocated emission of large amounts of  $C_2H_4$  and  $C_3H_6$  with  $NO_x$  from the isolated petrochemical facilities.

[23] Equally important in designing an effective  $O_3$  control strategy is the identification of VOC compounds that did not contribute significantly to OH reactivity, and thus prompt  $O_3$  formation, in the isolated plumes. While mixing ratios of many alkane compounds were enhanced, sometimes strongly, these contributed negligibly to  $O_3$  formation in the Freeport and Sweeny plumes on these timescales due to their substantially lower OH reaction rates. An exception is noted for the Chocolate Bayou plume, in which isobutane mixing ratios exceeding 20 ppbv were measured 5 km downwind, accounting for 11% of OH reactivity with the measured VOC compounds at this distance. Alkenes other than  $C_2H_4$  and  $C_3H_6$  contributed little to initial OH reactivity. While the OH rate coefficient for 1,3-butadiene is a factor of  $\sim 3$  larger than that for  $C_3H_6$  (Table 1), emissions of 1,3-butadiene contributed relatively little to OH reactivity in these plumes, even after accounting for differential loss in samples taken within 10 km of the Freeport and Chocolate Bayou facilities. All other directly emitted and individually measured VOCs contributed less than 0.2/s to the OH loss rate, and, to first approximation, can be neglected in terms of prompt  $O_3$  formation. This finding includes the suite of higher aromatic compounds measured (Table 1), which, like 1,3-butadiene, are very reactive, but were present at sufficiently low levels to be minor contributors to rapid  $O_3$  formation in the plumes presented here. Thus relatively few compounds were responsible for the bulk of initial VOC reactivity of these petrochemical plumes, which were dominated for the first 50 km of transport (first 2–3 hours after emission) by anthropogenic emissions of  $C_2H_4$  and  $C_3H_6$  and by the aldehyde photoproducts derived from these species. Enhancements in initial plume OH reactivity due to CO and  $NO_2$  emissions were negligible compared to the enhancements resulting from alkene emissions (Figure 3). Considering the wide variety of VOCs emitted from petrochemical industrial sources [Derwent, 2000], this finding suggests a relatively straightforward  $O_3$  control strategy. Reducing emission of these two alkenes is clearly indicated

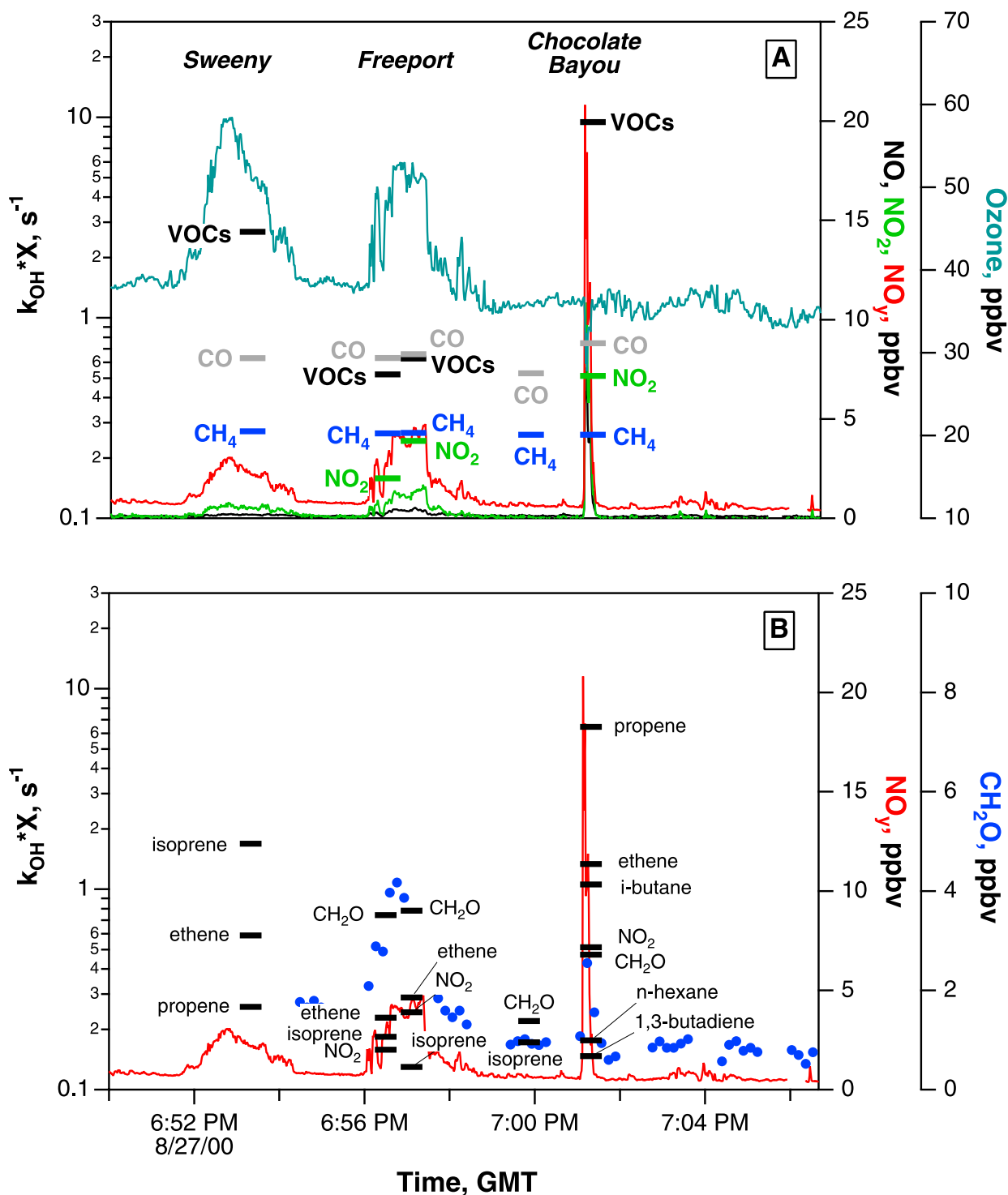


**Figure 3.** (a) Time series of chemical data from the aircraft transect at 29.3° latitude (Figure 2), which sampled plumes downwind of the Sweeny, Freeport, and Chocolate Bayou petrochemical complexes on 27 August 2000. Horizontal bars show the time, duration, and calculated value of  $k_{OH}X[NO_2]$  (green bars),  $k_{OH}X[CO]$  (gray bars),  $k_{OH}X[CH_4]$  (blue bars), and  $k_{OH}X[VOC]$  (black bars) for each hydrocarbon sample. (b) Speciated hydrocarbon measurements show that the alkenes ethene, propene, and isoprene account for >80%, and the sum of all measured aromatics <3%, of total plume OH reactivities with hydrocarbons on this transect. Derived loss rates for all measured volatile organic compounds (VOC) are plotted; note that most lie below the minimum y axis value of 0.1/s.  $CH_2O$  mixing ratios (blue circles) were sufficiently enhanced, primarily due to photoproduction from directly emitted alkenes, to represent a substantial reaction partner for OH in these plumes. (c and d) As in Figures 3a and 3b above, for the 29.3° latitude transect of the 28 August flight.

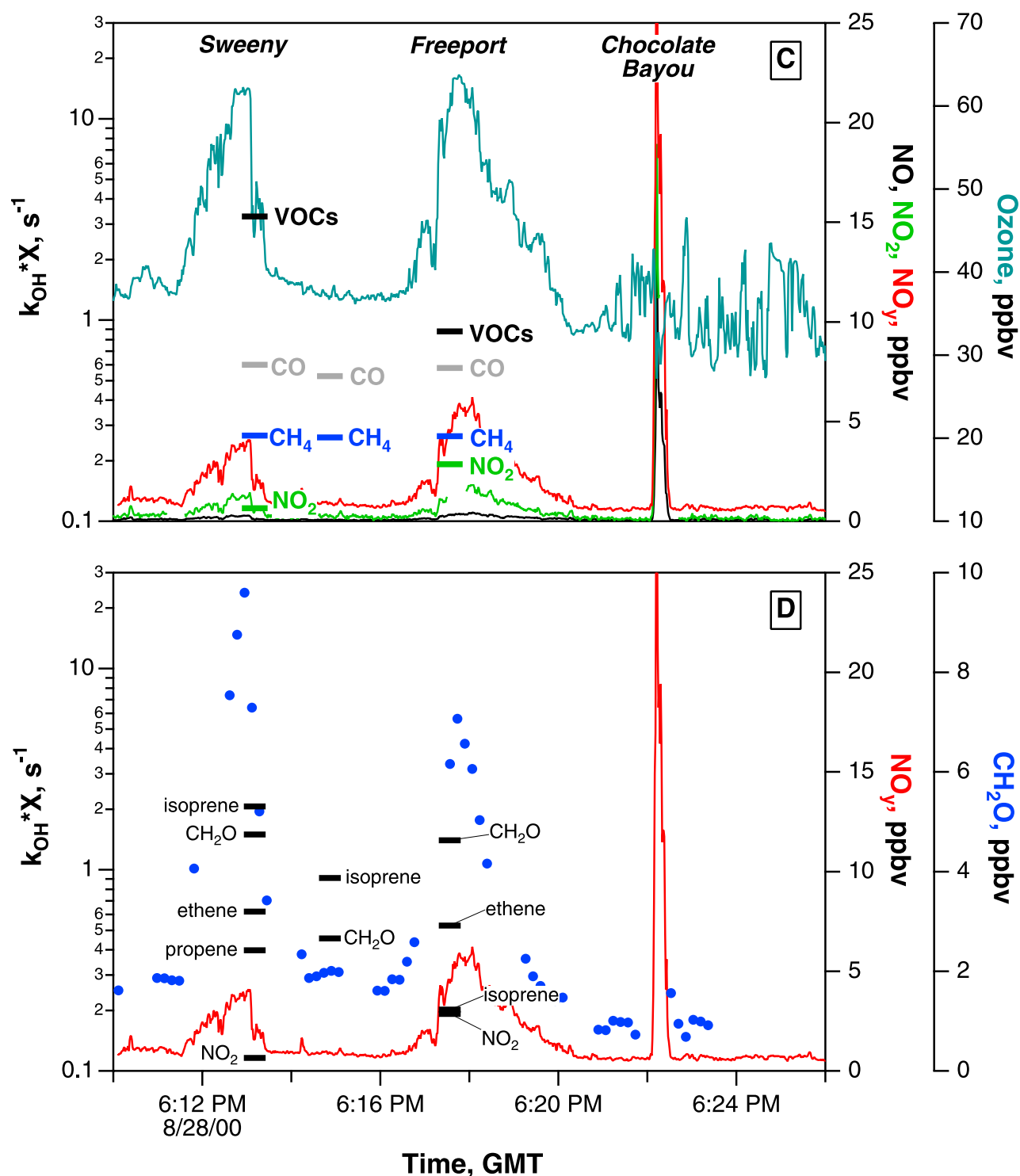


Figure 3. (continued)

as the most effective VOC-reduction strategy to minimize prompt  $O_3$  formation downwind of these sources.

### 3.1.3. (Alkene/ $NO_x$ ) Emission Ratios

[24] Ratios of coemitted species from a single large source are, to first order, independent of dilution over time during transport downwind and are given by the slope of a linear fit to measured data. Ratios measured downwind in plumes will differ from the emissions ratio if chemical

reaction or physical removal rates differ for the two species in question. We use plume transect data to estimate the emissions ratios of ( $C_2H_4/NO_x$ ) and ( $C_3H_6/NO_x$ ) for the Sweeny, Freeport, and Chocolate Bayou facilities, account for differential chemical loss with respect to OH, and compare to emissions ratios calculated from the 2000 TNRCC PSDB inventory. We note that some differences exist between the 1999 inventory used by *Wert et al.* [2003],

**Table 2.** Tabulated NO<sub>x</sub> and Alkene Emissions Rates and Ratios, and Measurement-Inferred Emission Ratios, for Selected Petrochemical Complexes and an Electric Utility Power Plant

Complex	$E_{\text{NO}_x}$ <sup>a</sup>	$E_{\text{ethene}}$ <sup>a</sup>	Tabulated Ethene/NO <sub>x</sub>	Measured Ethene/NO <sub>x</sub>	$E_{\text{propene}}$ <sup>a</sup>	Tabulated Propene/NO <sub>x</sub>	Measured Propene/NO <sub>x</sub>
Sweeny	12.6	0.6	0.05	3.6	0.4	0.03	2.0
Freeport	34.8	1.8	0.05	1.5	0.4	0.01	0.5
Chocolate Bayou	7.2	0.6	0.08	2.0	0.7	0.10	4.0
W.A. Parish	66.5	...	...	...	...	...	...

<sup>a</sup>Sum of annually averaged emissions (kmol/h) listed in the 2000 TNRCC PSDB for the boxes in Figure 1.

and the 2000 inventory used in the present work, which has only recently become available, for the Texas 2000 study period. These inventory tabulations are not static over time, reflecting changes in operating conditions, plant activity, and addition of new facilities or shutting down older units. Changes from the 1999 to the 2000 inventory are also due to a substantially smaller fraction of VOC emissions reported as “unspecified” in 2000. The PSDB inventory is the basis for the predictive and regulatory modeling by TNRCC and EPA.

[25] (C<sub>2</sub>H<sub>4</sub>/NO<sub>x</sub>) ratios measured in transects within 5 km of the Freeport and Chocolate Bayou facilities were not significantly affected by differential chemical or physical removal; the inferred emissions ratios are therefore judged to be accurate to within the combined measurement uncertainties of ±17%. The closest Sweeny plume transects took place ca. 22 km or 1.4 hours downwind; given the larger OH reaction rate for C<sub>3</sub>H<sub>6</sub> relative to NO<sub>x</sub> (Table 1); the resulting estimated (C<sub>3</sub>H<sub>6</sub>/NO<sub>x</sub>) emissions ratio is subject to the largest uncertainty. We judge the estimated (C<sub>3</sub>H<sub>6</sub>/NO<sub>x</sub>) emissions ratio for Sweeny is only accurate to within a factor of 2. These estimated emissions data are presented in Table 2 along with the ratios calculated from annual emissions rates listed in the 2000 PSDB inventory for the geographic source areas given by the rectangles in Figure 1. The data in Table 2 show that substantial discrepancies, many times larger than the measurement uncertainty, exist between the measurement-inferred emission ratios and those calculated from the 2000 inventory values. Small differences in the inventory (alkene/NO<sub>x</sub>) ratios between Table 2 in this report and those in Table 4 of *Wert et al.* [2003] are due to the different inventory reporting years.

[26] Such large discrepancies could arise from inaccuracy either in the tabulated inventory values of NO<sub>x</sub>, of alkenes, or of both, for the petrochemical complexes in question. The discrepancy could also arise if the actual NO<sub>x</sub> emissions were extremely low, or the alkene emissions extremely high, from all three facilities simultaneously during both the 27 and 28 August plume studies compared to the annual averages. In the following section, we show that the NO<sub>x</sub> emissions were relatively constant over time and are reasonably well estimated in the inventory.

### 3.1.3.1. NO<sub>x</sub> Emissions Were Constant Over Time

[27] The NO<sub>x</sub> emissions information is derived from CEMS data for many of the largest NO<sub>x</sub> sources at each complex; these data are believed to be accurate to better than ±30% on average [*Placet et al.*, 2000; *Ryerson et al.*, 1998]. Petrochemical facilities are typically operated continuously, so that variation in their NO<sub>x</sub> output over time can be minimal (C. Wyman, personal communication, 2001). As an example, total hourly averaged NO<sub>x</sub> emissions rates

reported by the largest of the four facilities in the Chocolate Bayou area differed by less than 5% for the 27 and 28 August plume study periods reported here. Further, very little variation is apparent over the 11 days of hourly averaged emissions rates for NO<sub>x</sub> (264 consecutive hours, average ± sigma = (7.9 ± 0.2), max = 8.5, min = 7.5, with units of 10<sup>23</sup> mol/s) reported by this facility (22 August–1 September 2000, including the plume study periods). The 2000 PSDB annually averaged NO<sub>x</sub> emissions rate is further consistent within 15% with that derived from the hourly averages from this facility. In addition, the available daily averaged NO<sub>x</sub> emissions data from the second largest facility show variations of less than 10% (11 consecutive days, average ± sigma = (2.7 ± 0.2), max = 3.0, min = 2.5, with units of 10<sup>23</sup> mol/s). Annual averages suggest these two facilities account for 91% of the total NO<sub>x</sub> emissions from the Chocolate Bayou source region. Similar arguments can be constructed for the facilities in the Sweeny and Freeport source regions (Figure 1). These findings suggest that for the 27 and 28 August plume studies, the emissions rates derived from hourly, daily, and annually averaged NO<sub>x</sub> inventories are comparable, and that NO<sub>x</sub> emissions from the three isolated petrochemical source regions were quite constant and representative of normal operating conditions of these complexes.

### 3.1.3.2. NO<sub>x</sub> Emissions are Well Represented by the Available Inventories

[28] The overall accuracy of the NO<sub>x</sub> emissions rates for these three complexes is evaluated by comparing to emissions rates inferred from plume mass flux of NO<sub>y</sub>, calculated from near-field aircraft transect data [*Brock et al.*, 2003; *Ryerson et al.*, 1998, 2001; *Trainer et al.*, 1995; *White et al.*, 1976], to the available inventory values. Mass flux estimates from aircraft data taken in well-resolved plumes are subject to several sources of uncertainty, including depositional losses, venting to the free troposphere, incomplete mixing within the boundary layer, and variability in wind speeds. These uncertainties and their evaluation are discussed extensively by *Ryerson et al.* [1998]. Examination of the multiple plume transect data on these 2 days suggests that the NO<sub>y</sub> mass flux was relatively well conserved over time. Plume NO<sub>y</sub>/SO<sub>2</sub> ratios remained constant, within ±30%, between successive transects on these 2 days (e.g., see *Brock et al.* [2003, Figure 8] for the analysis of the W.A. Parish plume), suggesting minimal differential loss of NO<sub>y</sub> relative to SO<sub>2</sub> and/or CO<sub>2</sub>. Further, the total estimated mass of NO<sub>y</sub> in each petrochemical plume remained constant within ±30% over time downwind of each complex, in turn suggesting that depositional loss of HNO<sub>3</sub> was relatively small compared to the total NO<sub>y</sub> on the timescales considered here. Thus NO<sub>y</sub> appears to have been approximately



conserved during the course of these plume studies. Given additional uncertainties in wind speed histories and boundary layer heights, for the isolated petrochemical plumes studied here, we conservatively estimate the uncertainty in derived  $\text{NO}_y$  mass flux to be a factor of 2. Comparison of the aircraft-derived  $\text{NO}_y$  flux estimates to the annually averaged  $\text{NO}_x$  inventory emissions values shows agreement within  $\pm 50\%$ , well within the uncertainty in deriving mass fluxes for these isolated facilities for these 2 days. This level of agreement rules out the inventory  $\text{NO}_x$  values as the primary source of inventory-measurement (alkene/ $\text{NO}_x$ ) ratio discrepancies of factors of 20 to nearly 70, mentioned above. These discrepancies are roughly a factor of 2 smaller than those noted in the work of *Wert et al.* [2003] using the 1999 PSDB inventory; while the total VOC emissions numbers remained approximately constant, more complete speciation in the 2000 inventory accounted for much of the change.

### 3.1.3.3. Alkene Emissions are Consistently Underestimated

[29] Inventory values of alkene emissions are therefore implicated as the primary cause of the large discrepancies in (alkene/ $\text{NO}_x$ ) emissions ratios. Hourly and daily  $\text{C}_2\text{H}_4$ ,  $\text{C}_3\text{H}_6$ , and butadiene emissions data from facilities in, e.g., the Chocolate Bayou source region suggest that total emissions of these alkenes showed minimal variability, within  $\pm 20\%$  of the average value over the 22 August–1 September time period, encompassing the two plume study days. Similarities observed between plumes sampled on 27 and 28 August, further consistent with the larger Electra data set from the monthlong Texas 2000 project, suggest that the instantaneous VOC emissions were representative of normal operations on both days and generally consistent with the annual average. No substantial upsets, or non-routine-emission events, were recorded for these facilities for the plume intercepts studied here. We conclude that consistently large discrepancies between measurement-derived and tabulated (alkene/ $\text{NO}_x$ ) ratios are due to consistently and substantially underestimated VOC emissions from the petrochemical facilities [*Wert et al.*, 2003].

### 3.1.4. $\text{NO}_x$ Oxidation Rate

[30] As discussed above, within  $\pm 30\%$  the measured  $\text{NO}_y$  was a reasonably conserved tracer of the  $\text{NO}_x$  originally emitted in these plumes. Any  $\text{NO}_y$  loss from the plumes would have biased derived  $\text{NO}_x$  oxidation rates to smaller-than-actual values, and  $\text{O}_3$  production rates and yields to larger-than-actual values. We assume that  $\text{NO}_y$  was conserved but present the derived  $\text{NO}_x$  oxidation rates as lower limits, and  $\text{O}_3$  rates and yields as upper limits, for plumes from the isolated petrochemical complexes.

[31] Slopes of linear least squares fits to measured  $\text{NO}_x$  versus  $\text{NO}_y$  from successive transects downwind are plotted in Figure 4a as a function of estimated transport time after emission [*Ryerson et al.*, 1998]. An average  $\text{NO}_x$  oxidation lifetime of  $1.5 \pm 0.5$  hours is derived from an exponential fit to the transect slope data, illustrating rapid photochemical processing of  $\text{NO}_x$  during transport downwind from all three sources on both days. Measured ( $\text{NO}_x/\text{NO}_y$ ) ratios  $> 2.5$  hours downwind were slightly elevated, relative to background ratios outside these plumes, likely due to entrainment of fresh emissions during transport over the edges of the Houston urban area. While this effect increases the

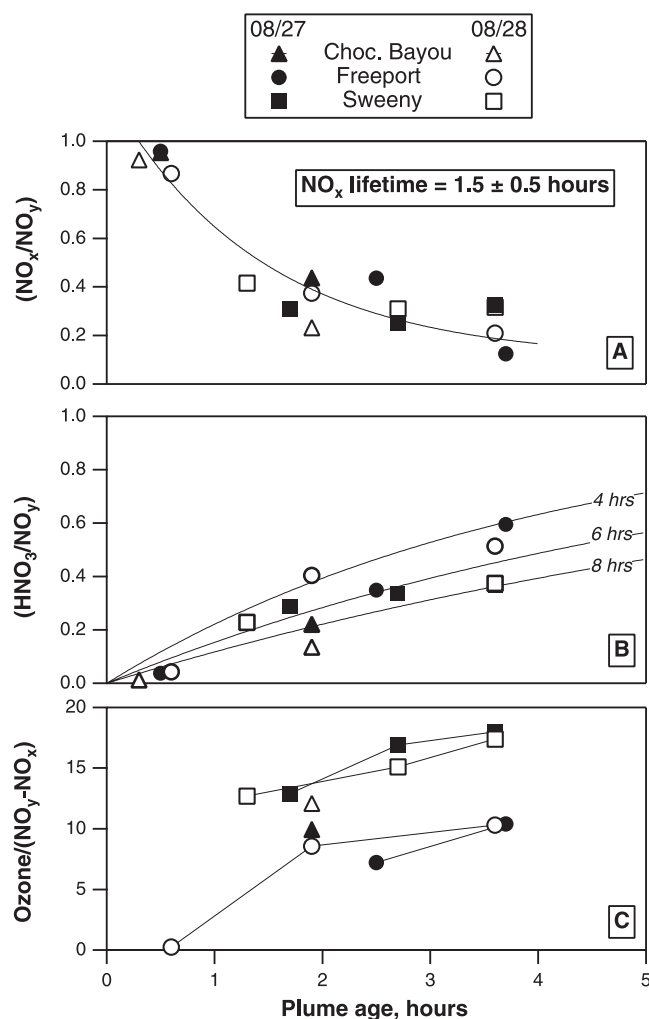


**Figure 4.** Data from isolated petrochemical plumes sampled on 27 and 28 August 2000. Plotted points are slopes derived from linear least squares fits to measured plume data. (a)  $\text{NO}_x$  lifetimes average 1.5 hours, suggesting rapid photochemical processing and strongly elevated plume  $\text{RO}_x$  and  $\text{OH}$  levels. (b)  $\text{HNO}_3$  formation over time. (c) Net ozone production yields of 10–18 mol/mol of  $\text{NO}_x$  oxidized are derived.

derived lifetime, a fit excluding these last points indicates a lifetime only 5% shorter.

[32] This derived lifetime of  $1.5 \pm 0.5$  hours reflects both  $\text{NO}_x$  oxidation via peroxy radical reaction, primarily leading to formation of PAN-type compounds with a minor fraction forming alkyl nitrates, and  $\text{NO}_x$  oxidation via  $\text{OH} + \text{NO}_2$  leading to formation of  $\text{HNO}_3$ .  $\text{HNO}_3$  accounted for roughly 50% of  $\text{NO}_y$  after several hours of transport (Figure 4b), with an approximately exponential risetime of 6 hours. In general, enhancements in PAN-type compounds, inferred from 1-Hz ( $\text{NO}_y - (\text{NO}_x + \text{HNO}_3)$ ) data, were substantial within the plumes, with peak contributions occurring sooner than for  $\text{HNO}_3$  and accounting for roughly 50% of plume  $\text{NO}_y$  at the peak.

[33] Previous studies of isolated, rural power plant plumes under midsummer afternoon, high Sun conditions with steady winds have reported  $\text{NO}_x$  lifetimes ranging



generally from 2 to 5 hours [Nunnermacker *et al.*, 2000; Ryerson *et al.*, 1998, 2001]. The range arises from differences in  $\text{NO}_x$  emissions rate (40–600 kmol/h; Table 3), variability in meteorological conditions determining plume dispersion rates, and availability of ambient reactive VOCs, principally isoprene. Together these factors have been shown to modulate the  $\text{NO}_x$  lifetime by over a factor of 2, with the shortest (2 hours) derived lifetimes observed in plumes from midsized ( $\sim 50$ – $100$  kmol/h) power plants emitted into a high isoprene background. The petrochemical plume  $\text{NO}_x$  oxidation reported here is presumed to proceed more rapidly due to initially mixed conditions arising from coemission of  $\text{NO}_x$  simultaneously with reactive VOCs.

### 3.1.5. Ozone Production Rate and Yield

[34] Prompt  $\text{O}_3$  formation downwind of these petrochemical facilities was observed on both days (Figures 2 and 4c). For example, enhancements of 20 ppbv in  $\text{O}_3$  were observed on the transects flown west-to-east at  $29.3^\circ$  latitude at 35 km downwind, or roughly 2 hours transport time, from the Freeport complex. These enhancements in mixing ratio are relatively modest, comparable to the increases in  $\text{O}_3$  observed in power plant plumes reported by Ryerson *et al.* [1998, 2001] and Nunnermacker *et al.* [2000], despite the generally lower  $\text{NO}_x$  emissions rates for the petrochemical sources. The modest mixing ratio increases were in part due to dilution of the plumes into a rapidly deepening mixed layer, from 400 m at the coast to over 1500 m at 25 km inland, as determined from airborne lidar measurements [Senff *et al.*, 1998] during the plume transects reported here. Given that  $\text{NO}_y$  appears to have been relatively well conserved in these plumes, we calculate a net  $\text{O}_3$  production efficiency, or yield, from the plume transect data [Trainer *et al.*, 1993].

[35] This calculation shows that while  $\text{O}_3$  mixing ratio enhancements were relatively small,  $\text{O}_3$  production rates and yields were high. Estimates of  $\text{O}_3$  yields per molecule of  $\text{NO}_x$  oxidized, derived from slopes of linear least squares fits to plume  $\text{O}_3$  versus ( $\text{NO}_y$ - $\text{NO}_x$ ) data [Trainer *et al.*, 1993], are plotted in Figure 4c as a function of time downwind for these three plumes for both days. Derived  $\text{O}_3$  yields ranged from 10 to 18 molecules of  $\text{O}_3$  produced per  $\text{NO}_x$  molecule oxidized. Similar  $\text{O}_3$  yield values are derived using plume-integrated amounts of  $\text{O}_3$  and ( $\text{NO}_y$  -  $\text{NO}_x$ ) according to a mass balance approach [e.g., Brock *et al.*, 2003; Ryerson *et al.*, 1998; Trainer *et al.*, 1995; White *et al.*, 1976]. These derived values were achieved very rapidly after emission, within roughly 2 hours for the isolated petrochemical plumes in Figure 4. The slow increases in derived yield after 2.5 hours in Figure 4c may be real, due to real  $\text{O}_3$  production from entrainment of fresh urban  $\text{NO}_x$  or to slower  $\text{O}_3$  production rates from longer-lived VOCs in the plume, or spurious, from nonnegligible depositional losses of  $\text{HNO}_3$  during transport. In any case, this effect is relatively minor for the short timescales and small changes in derived  $\text{O}_3$  yield after 2.5 hours observed here.

[36] While all plumes were consistent in producing ozone in high yield, differences between the Freeport and Sweeny plumes (Figure 4) are noted, with derived yields about 50% lower for Freeport. These differences are qualitatively consistent with different emissions rates of  $\text{C}_3\text{H}_6$  and  $\text{C}_2\text{H}_4$ , and (alkene/ $\text{NO}_x$ ) ratios, explored in the VOC reactivity section, above. In general, similarity between measured mixing

**Table 3.** Tabulated  $\text{NO}_x$  Emissions Rates for Electric Utility Power Plants in Figure 5

Power Plant	$E_{\text{NO}_x}$ <sup>a</sup>
Johnsonville, TN	40–65
Thomas Hill, MO	78
Cumberland, TN	300–600
Paradise, KY	350

<sup>a</sup>Data from continuous emissions monitoring systems at each plant, expressed as an annual average in kmol  $\text{NO}_2$ /h.

ratios and derived plume formation rates and yields for each complex on Sunday and Monday, with no upsets reported to TNRCC by the facility operators, implies the observed  $\text{O}_3$  production is representative of the effects of these facilities' routine emissions on tropospheric  $\text{O}_3$  mixing ratios downwind under these meteorological conditions.

#### 3.1.5.1. Uncertainties in Derived Ozone Yield (Resolved Plumes)

[37] Interpretation of  $\text{O}_3$ -to-( $\text{NO}_y$  -  $\text{NO}_x$ ) relationships in isolated, resolved plumes as a net  $\text{O}_3$  production yield is subject to several uncertainties, which are extensively discussed by Trainer *et al.* [1993] and Ryerson *et al.* [1998]. Of these,  $\text{NO}_y$  loss from these particular plumes during transport was a minor contributor, as discussed above. For the isolated and well-resolved petrochemical plumes from Sweeny, Freeport, and Chocolate Bayou, defining background mixing ratios immediately outside of the plumes is easily accomplished and introduces relatively little uncertainty in the derived  $\text{O}_3$  yields. Vertical profiles of chemical and meteorological data further support the assumption that the boundary layer was vertically well mixed, and that detrainment into the free troposphere was minimal, for these plumes within 5 hours of release.

[38] The most likely bias to the interpretation of the isolated petrochemical plume  $\text{O}_3$  and ( $\text{NO}_y$  -  $\text{NO}_x$ ) data as an apparent  $\text{O}_3$  production yield involves the use of a linear fit to inherently nonlinear relationships in the data [e.g., Liu *et al.*, 1987; Ryerson *et al.*, 1998, 2001; Sillman, 2000]. However, the ratio of plume-integrated  $\text{O}_3$  to plume-integrated ( $\text{NO}_y$  -  $\text{NO}_x$ ) assumes no particular relationship between the two data sets. Apparent  $\text{O}_3$  production yields for the isolated petrochemical plumes agree to better than  $\pm 50\%$  whether they are calculated from the slope of a linear fit, or from integrations, of the plume transect data [e.g., Ryerson *et al.*, 1998]. We therefore assign approximate but conservative uncertainties of  $\pm 50\%$  to the derived  $\text{O}_3$  yields for the isolated petrochemical plumes for these 2 days.

#### 3.1.5.2. Comparison to Power Plant and Urban Plumes

[39] Derived  $\text{O}_3$  yields are significantly higher and are attained more rapidly after emission in these resolved petrochemical plumes than are typically observed in rural power plant plumes [e.g., Gillani *et al.*, 1998; Nunnermacker *et al.*, 2000; Ryerson *et al.*, 1998, 2001]. This is attributed in part to the collocation of sources of anthropogenic  $\text{NO}_x$  with anthropogenic reactive VOCs, in distinct contrast to rural power plant plumes into which reactive VOCs must be entrained over time during transport [Luria *et al.*, 2000; Miller *et al.*, 1978; Ryerson *et al.*, 2001].

[40] For comparison purposes, the data in Figures 5a and 5b show  $\text{O}_3$  production rates and yields for several rural, isolated power plant plumes and for the Nashville, TN urban

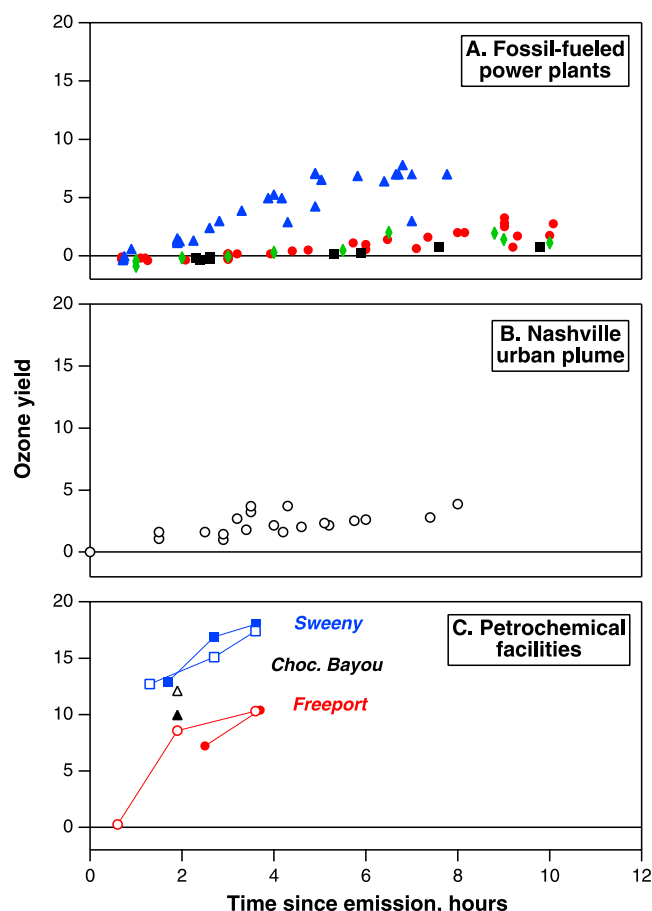


**Figure 5.** Derived ozone yields plotted as a function of time downwind for three anthropogenic source types. (a) Plume data from fossil-fueled power plants in Cumberland, TN (red circles, five flights in 1995 and 1999), Johnsonville, TN (blue triangles, four flights, 1995 and 1999), Paradise, KY (black squares, two flights, 1995), and Thomas Hill, MO (green diamonds, one flight, 1999). (b) The Nashville urban plume (five flights, 1995), and (c) plumes from the Sweeny (squares), Freeport (circles), and Chocolate Bayou (triangles) petrochemical complexes. The data in Figure 5c are reproduced from Figure 4c, with 27 August (solid symbols) and 28 August (open symbols) data shown.

plume, taken from multiple NOAA WP-3D aircraft research flights during the Southern Oxidants Study 1995 and 1999 field projects. Table 3 gives the  $\text{NO}_x$  emissions rates for the power plants included in Figure 5a. Petrochemical  $\text{O}_3$  yield data from Figure 4c are reproduced in Figure 5c. These data were all taken under approximately similar summertime afternoon high Sun conditions with relatively constant wind speeds between 4 and 5 m/s; all plumes were extensively oxidized at the final transects, with measured ( $\text{NO}_x/\text{NO}_y$ ) ratios of 0.25 or smaller. The data show scatter from day to day for a given plume, within the range expected from time-varying emissions rates, solar insolation, and meteorological conditions. Differences in  $\text{NO}_x$  emissions rates (Table 3) also affect  $\text{O}_3$  yields in these plumes. In general, however, the  $\text{NO}_x$ -rich power plant plumes take longer to fully

oxidize, and produce less  $\text{O}_3$  per unit  $\text{NO}_x$  oxidized, than do the urban plumes from Nashville [Daum *et al.*, 2000a; Nunnermacker *et al.*, 2000]. An exception is found in the Johnsonville plume, a midsized power plant located in a wooded area characterized by strong biogenic isoprene emissions. The Johnsonville plume typically experiences the highest  $\text{VOC}/\text{NO}_x$  ratios of the power plant plumes shown, with corresponding relative increases in  $\text{O}_3$  production rates and yields [Ryerson *et al.*, 1998, 2001]. The Nashville urban plume data were calculated from the slopes of linear fits to plume  $\text{O}_3$  versus  $\text{CO}$ , multiplied by an assumed urban  $\text{CO}/\text{NO}_x$  emissions ratio [Kleinman *et al.*, 1998; Parrish *et al.*, 2002]. The Nashville urban plume achieves a somewhat higher yield and does so more rapidly than most power plants studied to date. The petrochemical plumes, however, produce substantially more  $\text{O}_3$  per unit  $\text{NO}_x$ , and produce that  $\text{O}_3$  far more rapidly, than plumes from the other two anthropogenic source types compared here. Both the rapidity of formation and the eventual yield of  $\text{O}_3$  in these petrochemical plumes are qualitatively consistent with elevated mixing ratios of reactive VOCs and  $\text{NO}_x$  being initially present upon emission.

[41] Systematic differences in derived  $\text{O}_3$  yields between plumes from the three isolated petrochemical facilities are consistent with differences in source VOC profiles. The Sweeny plume was characterized by the highest initial ( $\text{C}_2\text{H}_4/\text{NO}_x$ ) ratio and showed the highest  $\text{O}_3$  yields of the three plumes studied here. The additional entrainment of biogenic isoprene into the Sweeny plume during transport also tends to increase the  $\text{O}_3$  yield. The Freeport plume exhibited the lowest (alkene/ $\text{NO}_x$ ) ratios and consequently showed slightly lower  $\text{O}_3$  yields than plumes from the other two facilities. Real differences exist in petrochemical source emissions profiles, so that generalization from this study to all petrochemical industrial emissions is not warranted. Plumes from gasoline refineries, for example, are primarily composed of alkanes and are low in reactive alkenes [e.g., Kalabokas *et al.*, 2001; Sexton and Westberg, 1979, 1983; Watson *et al.*, 2001]; these typically do not produce  $\text{O}_3$  as rapidly or in as high a yield.

### 3.1.6. Contrast to Initial OH Reactivity in a Power Plant Plume

[42] The  $\text{OH} + \text{alkene}$  reactions described above initiate radical chain propagation steps that result in substantial net  $\text{O}_3$  formation downwind. The radical chain termination step of  $\text{NO}_2 + \text{OH}$  is seen to be of lesser importance soon after emission (Figures 3b and 3d), confirming that overall radical chain lengths are relatively long at the high ( $\text{VOC}/\text{NO}_x$ ) ratios characteristic of these petrochemical industrial plumes. The apparent yield of 10–18 molecules of  $\text{O}_3$  per  $\text{NO}_x$  molecule oxidized from these complexes is qualitatively consistent with the extended radical chain length deduced from initial hydrocarbon reactivity (e.g., Figure 3) [Derwent and Davies, 1994]. In contrast, in the  $\text{NO}_x$ -rich and VOC-poor plume from the W.A. Parish electric utility power plant,  $\text{NO}_2$  is the primary OH reaction partner immediately downwind (Figure 6), favoring  $\text{HNO}_3$  formation in the early stages of plume transport [Neuman *et al.*, 2002; Ryerson *et al.*, 2001]. Slower rates of  $\text{O}_3$  formation and lower eventual  $\text{O}_3$  yields are predicted for the Parish plume on the basis of the data shown in Figure 6. We present the derived  $\text{O}_3$  yield in the aged Parish plume along

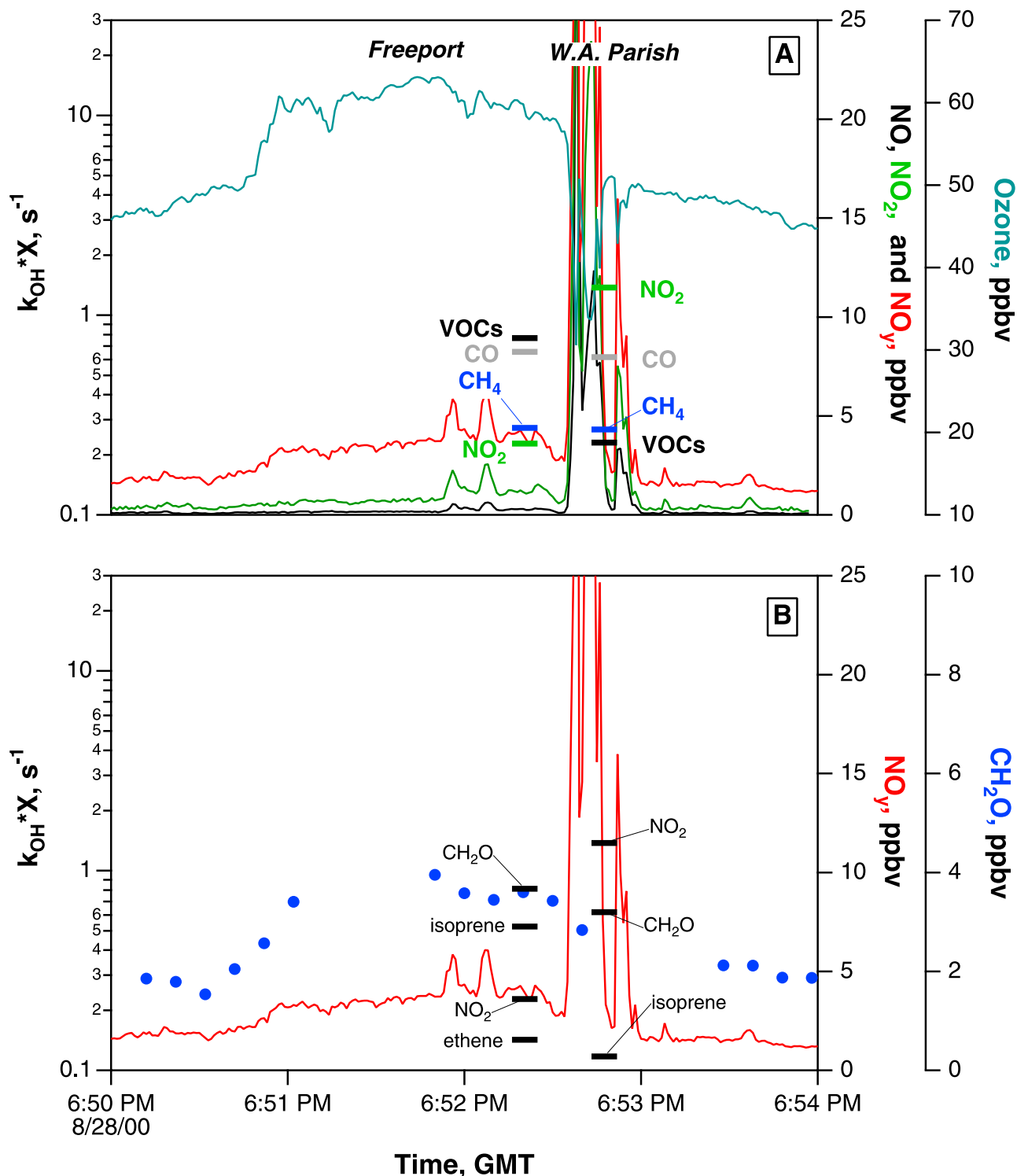


**Figure 6.** As in Figure 4 for the 28 August flight data, from the aircraft transect at 29.5° latitude roughly 4 km downwind of the W.A. Parish power plant. The broad maximum in ozone resulted from photochemically aged emissions from the Freeport petrochemical complex, into which the Parish plume, here defined by NO > 1 ppbv, was emitted. The data show the OH + NO<sub>2</sub> radical termination step leading to HNO<sub>3</sub> formation was strongly favored in the Parish plume at this transect.

with those from the Ship Channel petrochemical industrial sources and the Houston urban area in section 3.2 below.

### 3.2. Comparison of Anthropogenic Source Types: Petrochemical, Urban, and Power Plant

[43] The Electra flights of 27 and 28 August also sampled the coalesced plume from multiple petrochemical complexes to the southeast and east of Houston, the plume from the Houston urban core, and that from the W.A. Parish gas- and coal-fired power plant (Figure 1). Steady southerly winds on both days led to transport of anthropogenic  $\text{NO}_x$  and VOC emissions from facilities in Texas City toward and over other substantial petrochemical sources located in LaPorte, Deer Park, Pasadena, Channelview, and Baytown, all generally adjacent to the Houston Ship Channel roughly 40 km north of Texas City (Figure 1). Each complex encompasses a large number of individual facilities in close proximity, each with potentially unique emissions with differing ratios of VOCs to  $\text{NO}_x$ , complicating transect-by-transect analysis of individual source emissions plumes. Transport times on the order of hours over this extended grouping of petrochemical sources further complicates process analysis similar to that employed for the isolated petrochemical plumes, above, which requires knowledge of transport time. In contrast to the isolated plumes, photochemical processing in the coalesced Texas City/Ship Channel plume air parcels on these 2 days was repeatedly affected by substantial injections of fresh emissions during transport over source locations downwind. While near-field transect data are sufficient to distinguish individual sources, mixing during transport quickly acted to diminish individual plume signatures.

[44] We focus on data taken in photochemically aged plumes downwind of the respective source regions to illustrate the net cumulative effect of multiple upwind sources on  $\text{O}_3$  formation rate and yield. The northernmost transects were flown east-to-west at  $30.3^\circ$  latitude or 70 km north of the Ship Channel on 27 August ( $30.6^\circ$  or 90 km on 28 August) and were characterized by a plume  $\text{NO}_x/\text{NO}_y$  ratio of roughly 0.20, indicating that  $\sim 80\%$  of the original  $\text{NO}_x$  emissions had been oxidized at this distance downwind. During these transects, no single petrochemical point source was clearly distinguishable in the time series, while broad enhancements in oxidized nitrogen species,  $\text{O}_3$ , CO,  $\text{CO}_2$ , and  $\text{SO}_2$  were all well correlated due to extensive mixing and reaction of plume constituents from multiple petrochemical point sources upwind. We analyze data from two transects, one at  $\sim 2.7$  hours and the other  $\sim 5.6$  hours downwind of the Ship Channel, to extract information on differences in  $\text{O}_3$  formation rates and yields between the three source types.

#### 3.2.1. Coalesced Petrochemical Plumes

##### 3.2.1.1. Contribution of Petrochemical Emissions to Observed $\text{NO}_x$ Mixing Ratios

[45] Comparisons of the observed petrochemical source region  $\text{CO}/\text{NO}_x$  ratios to those from other urban areas [e.g., Harley *et al.*, 2001; Kleinman *et al.*, 1998; Parrish *et al.*, 1991, 2002] and to that in the Houston urban core imply that petrochemical  $\text{NO}_x$  emissions contributed substantially to the elevated  $\text{NO}_x$  mixing ratios typically observed in the Ship Channel plume. The magnitudes of the largest enhancements in  $\text{NO}_x$ ,  $\text{CO}_2$ , and  $\text{SO}_2$ , as well as their tight

correlations, are characteristic of natural gas- or oil-fired point sources and are quite different than those typically observed as a result of tailpipe emissions alone. However, the contribution of  $\text{NO}_x$  emitted from typically urban mobile sources in this area was not negligible in terms of  $\text{O}_3$  formation in these coalesced plumes. Observed  $\text{O}_3$  downwind of the Ship Channel on 27 and 28 August is therefore interpreted as the net effect of photochemical processing of  $\text{NO}_x$  emissions from both petrochemical and urban  $\text{NO}_x$  sources.

##### 3.2.1.2. Contribution of Petrochemical Emissions to Observed VOC Mixing Ratios

[46] ( $\text{C}_3\text{H}_6$ /ethyne) and ( $\text{C}_2\text{H}_4$ /ethyne) ratios above and immediately downwind of the Ship Channel and Texas City source areas ranged from 5 to 40 and from 3 to 40, respectively. These ratios are consistent with those in resolved plumes from geographically isolated petrochemical sources south of Houston, discussed above, suggesting that elevated mixing ratios of reactive alkenes in the coalesced Ship Channel plume are primarily due to emissions from the petrochemical industry. We conclude that on-road tailpipe emissions were insignificant contributors to the observed alkene mixing ratio enhancements, and thus the bulk of VOC reactivity determining  $\text{O}_3$  formation, despite the general location of petrochemical sources within the extended Houston metropolitan area. The resulting prompt  $\text{O}_3$  formation is primarily ascribed to emissions of  $\text{C}_3\text{H}_6$  and  $\text{C}_2\text{H}_4$  from Ship Channel petrochemical industrial sources, with relatively minor contributions from urban VOCs on the timescales considered here.

##### 3.2.1.3. Initial VOC Reactivity

[47] Aircraft measurements on 27 and 28 August show that the primary OH reactivity in the coalesced petrochemical plume beginning north of Texas City and extending downwind over and past the Ship Channel was due to reaction with petrochemical emissions of reactive alkenes and their photoproducts  $\text{CH}_2\text{O}$  and  $\text{CH}_3\text{CHO}$ . Because of the limited number of VOC samples on any single flight, this conclusion is best illustrated using the full data set from all 14 Electra research flights in the Houston area (Figure 7). Derived total OH loss rates to measured VOC compounds from in situ and canister measurements within the boundary layer during the 2000 Houston study are plotted (circles) as a function of sampling location in Figure 7. The symbols in Figure 7 are sized by the magnitude of OH reactivity with measured VOCs and colored by the fractional contribution of alkenes to the total reactivity.

[48] The data shown in Figure 7 demonstrate that OH reactivity from the measured VOC compounds was substantially enhanced above the petrochemical source regions relative to the urban area or the surrounding rural areas. Emissions plumes were encountered in different directions downwind depending on the prevailing wind direction on a particular day; for example, in Figure 7 the Texas City plume enhancements can be found both east over Galveston Bay, or west and inland. Independent of wind direction, the maximum reactivity on every flight was clearly localized over the Ship Channel. The samples in the Sweeny, Freeport, and Chocolate Bayou plumes on 27 and 28 August, discussed above, are included in Figure 7, but show relatively low reactivity compared to the Ship Channel region. Alkenes strongly dominated the total reactivity.



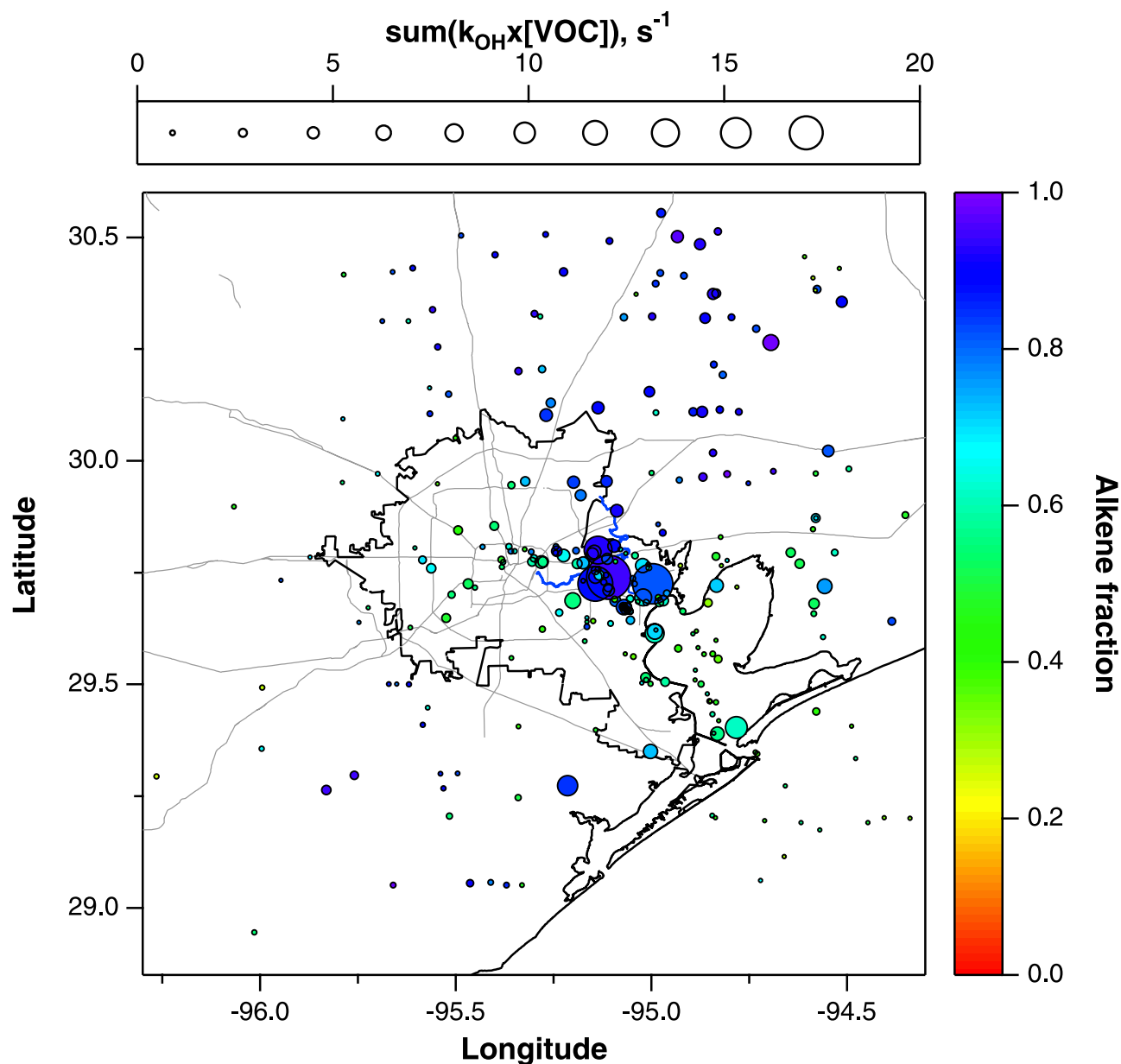


**Figure 7.** A  $200 \times 200$  km map of the study area showing locations of in situ and whole-air canister hydrocarbon measurements (circles) taken below 1.5 km aircraft altitude, sized by  $\Sigma (k_{\text{OH}}X[\text{VOC}])$  and colored by  $(\Sigma(k_{\text{OH}}X[\text{alkene}]))/(\Sigma(k_{\text{OH}}X[\text{VOC}])),$  the fractional contribution of alkenes to the total.

Above the Ship Channel, the contribution from alkenes was typically  $>80\%$  (Figure 7). The contribution from elevated mixing ratios of  $\text{C}_3\text{H}_6$  and  $\text{C}_2\text{H}_4$  dominated, with the two compounds constituting  $>70\%$  of the measured total directly over the source areas. Generally,  $\text{C}_3\text{H}_6$  contributed a factor of approximately 2 more than  $\text{C}_2\text{H}_4$  did, and all other alkenes contributed substantially less, to derived OH reactivity in the Ship Channel source region.

[49] The remainder of alkene reactivity was primarily due to isoprene, likely from a combination of anthropogenic and biogenic sources, and 1,3-butadiene; however, on average these dienes contributed less than 10% of the Ship Channel total. Samples taken immediately downwind of the Texas City petrochemical complexes suggest proportionally

greater contributions from the branched alkanes 2-methylpropane and 2-methylbutane, but these did not exceed 10% of the total calculated OH reactivity close to the source region. Given the varied nature of the petrochemical industrial facilities in the Houston area, other compounds were occasionally substantially enhanced, presumably when a VOC sample was taken very close to an individual source of that particular compound. With few exceptions, however,  $\text{C}_3\text{H}_6$  and  $\text{C}_2\text{H}_4$  dominated the reactivity toward OH of the emissions mix from the petrochemical industry in this area.

[50] In contrast to the Ship Channel area, measurements taken in the Houston urban core exhibited substantially lower OH reactivity, with values typically  $<2.0/\text{s}$  and similar



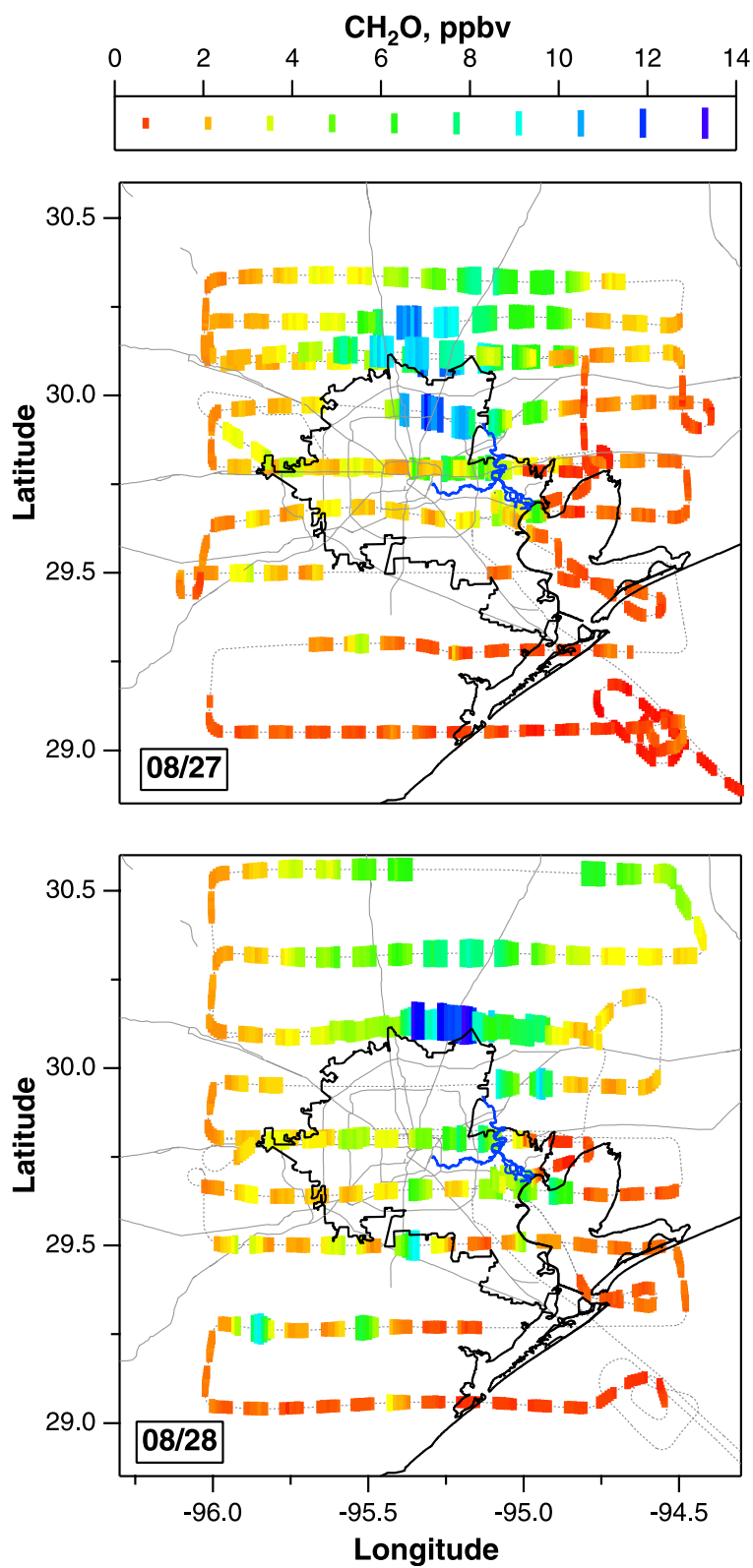


**Figure 8.** Map showing  $\text{CH}_2\text{O}$  (bars) measured below 2 km altitude along Electra flight tracks of 27 August (first panel) and 28 August (second panel).  $\text{CH}_2\text{O}$  mixing ratios are given by the size and color of the vertical bars, according to the legend at top. Direct emissions of  $\text{CH}_2\text{O}$  are seen to be negligible compared to that produced from alkene + OH reactions during transport downwind.

to that of other major urban areas studied to date. While a major fraction of reactivity in the urban core is due to alkenes emitted from transportation sources, the resulting mixing ratios were sufficiently low that the total OH reactivity was small compared to air masses sampled directly over petrochemical source regions in the Ship Channel.

[51] Enhancements in  $C_3H_6$  and  $C_2H_4$  dominated OH reactivity above the petrochemical source regions, but these compounds are sufficiently reactive that daytime atmospheric mixing ratios decay rapidly with distance downwind (Figure 7). Photooxidation of these reactive alkenes produces  $CH_2O$  and  $CH_3CHO$ , which are themselves quite reactive and are also subject to photolysis, further propagating the  $HO_x$  radical chain.  $CH_2O$  data measured aboard the Electra on the 27 and 28 August flights are shown as a function of aircraft location in Figure 8. Minimal enhancements above petrochemical source regions suggest that while some direct emissions are possible, the bulk of the observed  $CH_2O$  on 27 and 28 August was formed as a secondary product of alkene oxidation downwind of petrochemical complexes [Wert *et al.*, 2003]. The enhancements of  $CH_2O$  at intermediate distances downwind of the Sweeny and Freeport facilities shown in the time series of Figures 3b and 3d are also apparent in Figure 7b. Decreases in  $CH_2O$  mixing ratios observed further downwind are also consistent with very short-lived alkene species as the primary  $CH_2O$  source. As source alkenes rapidly reacted away (Figure 7),  $CH_2O$  mixing ratios first increased, then decreased with distance downwind (Figure 8) as the alkene source was consumed, and  $CH_2O$  loss and plume dilution acted to decrease atmospheric mixing ratios thereafter [Wert *et al.*, 2003]. On-board measurements of  $CH_3CHO$  (P. Goldan, manuscript in preparation, 2003), while more limited in coverage, are generally consistent with the interpretation of VOC and  $CH_2O$  data presented above. Thus on the flights of the 27 and 28 August, the bulk of the measured VOC reactivity in coalesced plumes from Texas City and the Houston Ship Channel was due to substantial petrochemical emissions of  $C_3H_6$  and  $C_2H_4$  and their photoproducts  $CH_2O$  and  $CH_3CHO$ . Again, no substantial upsets involving  $C_3H_6$  or  $C_2H_4$  releases coincident with the aircraft transects were reported to TNRCC on either of these 2 days, suggesting that the observations are representative of the averaged impact of routine petrochemical industrial operations in this area.

#### 3.2.1.4. Ozone Formation Rate and Yield in the Coalesced Petrochemical Plume

[52]  $O_3$  production takes place rapidly in the coalesced plume downwind of the Ship Channel industrial facilities, consistent with the findings from the isolated petrochemical plumes discussed above. This is illustrated by a time series of  $O_3$  data taken along the E-W transect at  $30.1^\circ$  latitude within the boundary layer (Figure 9). Plume locations from sources in the Ship Channel (blue line, in inset map in Figure 9), the Houston urban area (red line), and the W.A. Parish power plant (black circle) are shown as heavy overlays along the flight track (dotted line). The upper time series in Figure 9 shows the directly emitted compounds  $NO_3$ ,  $CO_2$ , and  $CO$ ; these tracers and  $SO_2$  (not shown) were used to differentiate between the various plumes, whose edges are approximately defined by the vertical dashed

lines. The lower time series shows the photoproducts  $O_3$  and  $CH_2O$  measured along this transect, which was flown approximately 43 km north, or 2.7 hours transport time, downwind of the Ship Channel and the I-10 corridor just north of downtown Houston.

[53] Differences are apparent between the three plumes in the amount of  $O_3$  produced by this time downwind. Petrochemical plume mixing ratios of  $O_3$  approaching 140 ppbv were coincident with  $CH_2O$  of 14 ppbv, which were the highest values for either species encountered during this flight; much smaller enhancements are found in the urban and power plant plumes. Differences in  $NO_y$  mixing ratios between the three plumes were much less pronounced (Figure 9, first panel), suggesting that the rapidity of  $O_3$  formation was primarily due to the enhanced VOC reactivity characteristic of Houston-area petrochemical emissions. Rapid  $O_3$  production leading to the accumulation of very high, spatially localized surface  $O_3$  mixing ratios has been a unique feature of the Houston area; these findings point toward petrochemical industrial emissions as the primary cause of the observed high  $O_3$  events.

[54]  $O_3$  formation yield is inferred from data taken in the most fully oxidized transects downwind. The geographical extent of the photochemically processed Ship Channel/Texas City plume on 28 August is defined by substantial enhancements in  $CO_2$  and  $SO_2$ , with relatively smaller enhancements in  $CO$ , observed on the northernmost transect downwind (Figure 10 inset). At this transect,  $\sim 5.6$  hours downwind of the Ship Channel, the coalesced petrochemical plume ( $NO_x/NO_y$ ) ratio was  $0.19 \pm 0.02$ , indicating extensive photooxidation of primary  $NO$  emissions had occurred during transport. Coalesced petrochemical plume  $O_3$  data from this transect are plotted in Figure 9a versus measured ( $NO_y - NO_x$ ). These data are highly correlated ( $r^2 = 0.978$ ) with a linear least squares fitted slope suggesting that, neglecting depositional loss of  $HNO_3$  during transport, roughly 12 molecules of  $O_3$  had been generated per  $NO_x$  molecule oxidized [Trainer *et al.*, 1993] at this distance downwind on 28 August. For comparison, a slope of 11 is derived from  $O_3$  plotted versus ( $NO_y - NO_x$ ) using the 27 August flight data from the northernmost transect, showing consistency from day-to-day. These high apparent yields are consistent with the range of  $O_3$  yields derived using data from the isolated and resolved plumes from the petrochemical complexes at Sweeny, Freeport, and Chocolate Bayou, described above. Again, these derived yields are substantially larger than recent measurements suggest for both urban and power plant plumes, reflecting the extremely reactive mix of VOC and the elevated ( $VOC/NO_x$ ) ratios in plumes from petrochemical industrial complexes in the Houston area. Similarity in derived  $O_3$  yields between the 2 days, with no substantial emission upsets reported to TNRCC, indicates these values are representative for emissions during normal operation of the multiple Ship Channel and Texas City petrochemical complexes under the meteorological conditions of those 2 days.

[55] We note that the derived yields exceeding 10 mol/mol for the petrochemical plumes encountered on 27 and 28 August are some of the highest values calculated from the Electra data set during the Texas 2000 project. Lower  $O_3$  yields are derived in the more concentrated plumes that lead to the highest  $O_3$  mixing ratios, from 150 to over 200 ppbv

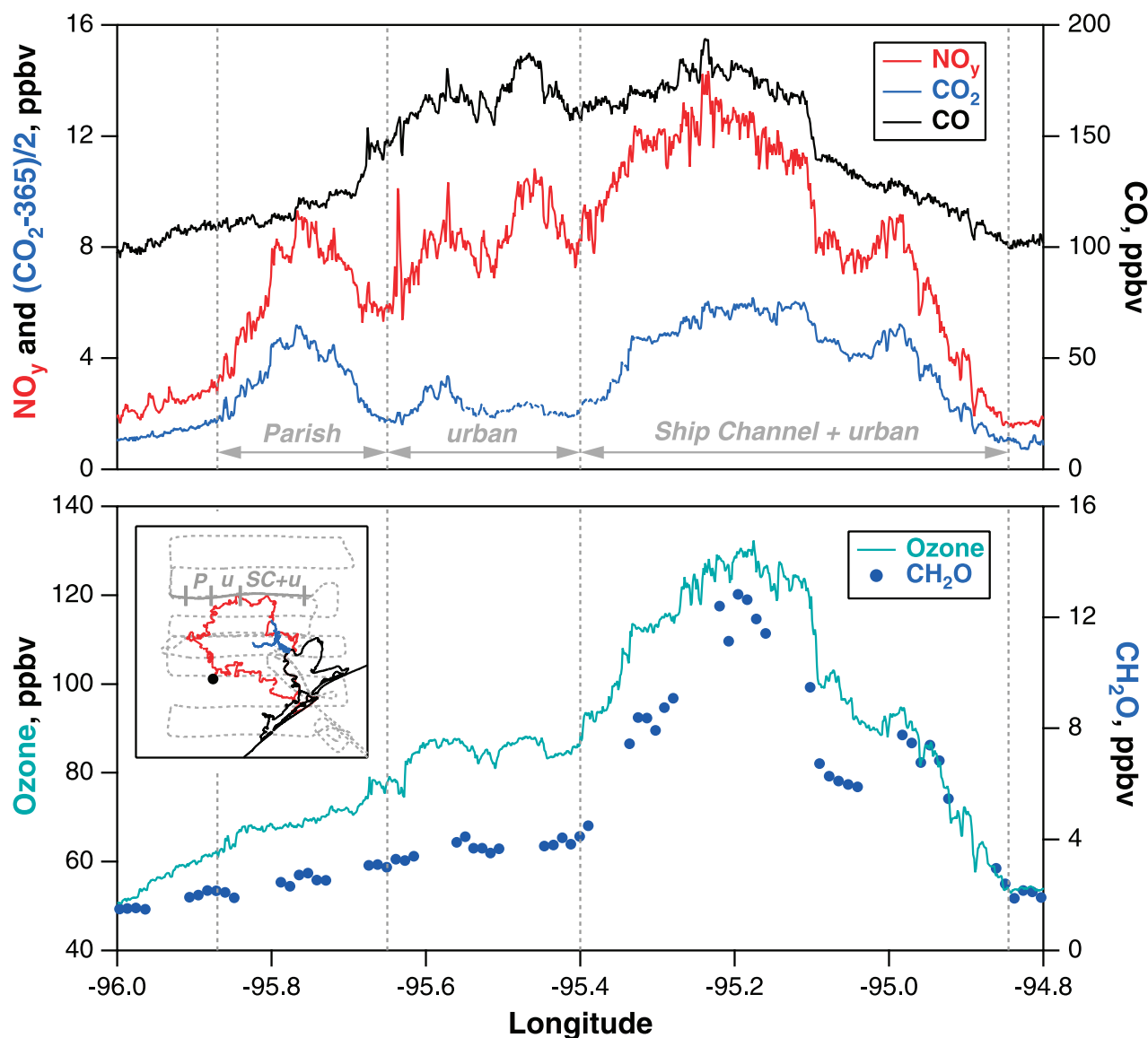


**Figure 9.** The inset map shows the E-W transect at  $30.1^\circ$  latitude on 28 August 2000 (solid gray line) along the aircraft flight track (dotted gray line). Locations of plumes from the W.A. Parish power plant “P,” the Houston urban core “u,” and the combined Ship Channel and urban plume “SC + u” along this transect are indicated by the vertical lines in the inset map and in the time series.

of  $\text{O}_3$ , during the extreme  $\text{O}_3$  exceedence episodes observed from the Electra aircraft. More rapid plume dilution, under the meteorological conditions of 27 and 28 August, likely increased the  $\text{O}_3$  formation yield in the plumes considered in this report; this is qualitatively consistent with the expected dependence of  $\text{O}_3$  formation yield on plume  $\text{NO}_x$  concentration [e.g., Derwent and Davies, 1994; Liu et al., 1987; Ryerson et al., 2001]. Slower rates of dilution are expected to both decrease  $\text{O}_3$  yield and permit higher  $\text{O}_3$  mixing ratios to accumulate. In addition, the prevailing wind direction has a substantial effect on atmospheric concentrations resulting from Ship Channel petrochemical emissions. N-S winds perpendicular to the Ship Channel axis, such as on 27 and 28 August 2000, will advect a given air parcel much more rapidly over the petrochemical source

region than will E-W winds blowing along the long axis of the Ship Channel (Figure 1). Other things being equal, different atmospheric mixing ratios due to different prevailing wind directions will therefore modulate  $\text{O}_3$  formation rates and yields downwind.

### 3.2.2. Ozone Yields in the Houston Urban Plume

[56] The relatively undisturbed Houston urban plume is defined by a maximum in  $\text{CO}$ , the relative minimum in  $\text{CO}_2$ , and the absence of measurable  $\text{SO}_2$  found between the coalesced Ship Channel/Texas City plume and the Parish power plant plume on transects from both days. While these segments do not encompass the entire urban plume, they are sufficient to define an approximately linear trend in  $\text{O}_3$  versus measured  $(\text{NO}_y - \text{NO}_x)$ , plotted in Figure 10a from the northernmost transect on 28 August. These urban plume

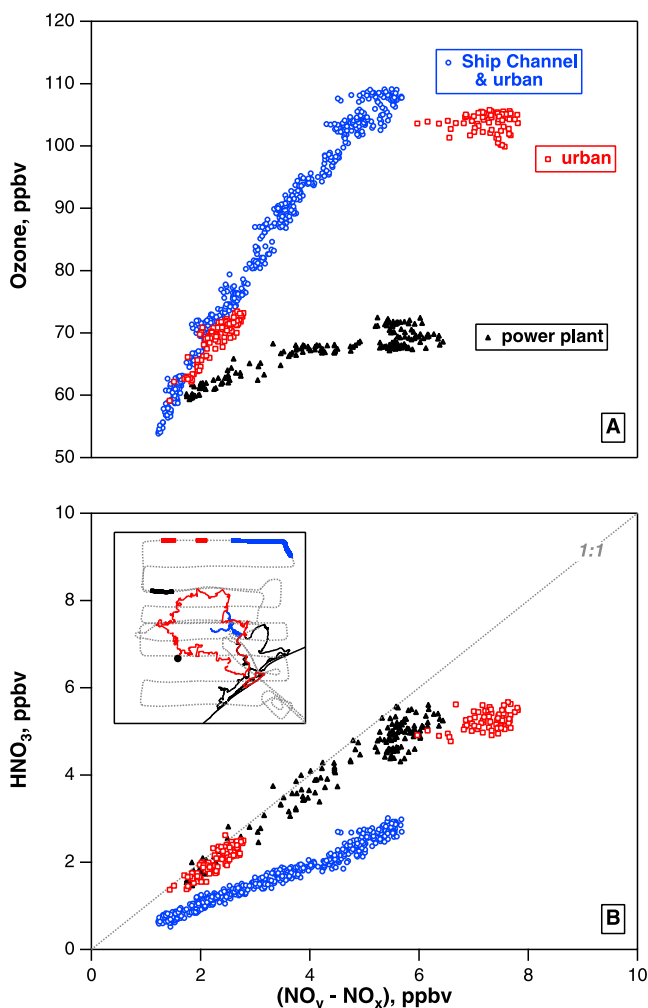


**Figure 10.** Transect data for the W.A. Parish (black,  $\text{NO}_x/\text{NO}_y = 0.24$ ), Houston urban (red,  $\text{NO}_x/\text{NO}_y = 0.19$ ), and Ship Channel/Texas City petrochemical plumes (blue,  $\text{NO}_x/\text{NO}_y = 0.19$ ) for 28 August flight. Location of these plume transects are given by the colored overlays along the flight track shown in the inset map. Markedly different enhancements in ozone as a function of  $\text{NO}_x$  oxidized are apparent (a), consistent with initial  $\text{VOC}/\text{NO}_x$  ratios observed immediately downwind of the sources and with large differences in the fraction of  $\text{HNO}_3$  generated (b) at these distances downwind.

data were characterized by a  $\text{NO}_x/\text{NO}_y$  ratio of  $0.19 \pm 0.03$ , virtually identical to that observed in the Ship Channel plume, suggesting a roughly similar extent of photochemical processing and facilitating direct comparison of derived  $\text{O}_3$  yields at this transect. The  $\text{O}_3$  yield of  $5.4 \pm 0.2$  derived from a fitted slope to the Houston urban plume data in Figure 10a is consistent with the range of reported yields for other urban areas [e.g., Daum *et al.*, 2000a; Nunnermacker *et al.*, 2000; Trainer *et al.*, 1995] (see also Figure 5b). The yield in the Houston urban plume is found to be a factor of  $\sim 2$  lower than that derived for the Ship Channel plume along the same transect at similar levels of  $\text{NO}_x$  oxidized. The difference resulted from substantially different proportions of  $\text{NO}_x$  oxidation by OH relative to oxidation by

peroxy radicals integrated over the transport history of each plume.

### 3.2.3. Ozone Yields in the W.A. Parish Power Plant Plume

[57] The Parish plume transect characterized by a  $\text{NO}_x/\text{NO}_y$  ratio of  $0.24 \pm 0.04$  was sampled at  $30.1^\circ$  latitude on 28 August, or two transects south of that used to derive Ship Channel and Houston urban plume  $\text{O}_3$  yields. The derived  $\text{O}_3$  yield from the slope of the power plant plume transect data in Figure 10a is  $2.2 \pm 0.2$ . The Parish plume had been emitted into the aged plume from the Freeport complex upwind and was later advected over the western edge of the Houston metropolitan area. Despite these external sources of hydrocarbons, the Parish plume ( $\text{VOC}/\text{NO}_x$ ) ratio (Figure 6) during transport was apparently sufficiently low that relatively little  $\text{O}_3$  had been formed by the transect shown in Figure 10a. This finding is consistent with the prediction of low  $\text{O}_3$  yield from the low ( $\text{VOC}/\text{NO}_x$ ) ratio observed just after emission, noted above (Figure 6). The factor of  $\sim 2$  difference in observed  $\text{O}_3$  yields between the Parish power plant and the Houston urban plumes at similar ( $\text{NO}_x/\text{NO}_y$ ) on the 28 August, and a factor of over  $\sim 5$  between the Parish and the Ship Channel plumes, is ascribed to the combined effects of substantial source differences in  $\text{NO}_x$  and  $\text{VOC}$  emissions rates, the resulting plume mixing ratios, and ( $\text{VOC}/\text{NO}_x$ ) ratios between plumes from these three anthropogenic types.

[58] Ozone production rates and yields are dependent on a number of factors, including rates of dispersion and mixing determined by the meteorological situation on a particular day. Aircraft observations on other days during the Texas 2000 study show different derived rates and yields in plumes from the sources considered here. Thus while the relative differences between  $\text{O}_3$  production in plumes from different sources remain, absolute values of  $\text{O}_3$  production rate and yield reported here will vary with insolation or meteorology.

#### 3.2.3.1. Uncertainties in Derived Ozone Yields (Overlapping Plumes)

[59] While  $\text{HNO}_3$  loss has been shown to be relatively modest ( $<20\%$  in 4 hours) for the isolated petrochemical facilities and the W.A. Parish plumes on 27 and 28 August, the extent to which this process affected measured  $\text{NO}_y$  mixing ratios in the overlapping Ship Channel and urban plumes is not known. However, at the earlier transects (e.g., at  $30.1^\circ$  latitude, 2.7-hours-old, Figure 9) when potential  $\text{NO}_y$  loss is thought to be less significant, the apparent  $\text{O}_3$  production efficiency had already reached 9 mol/mol in the Ship Channel plume. Another confounding factor in interpreting fitted slopes to measured  $\text{O}_3$  and ( $\text{NO}_y - \text{NO}_x$ ) data solely in terms of photochemical  $\text{O}_3$  production comes from variability in the background due to partially overlapping plumes. Given the uncertainties in estimating  $\text{O}_3$  yields from measured data in partially overlapping plumes, the apparent  $\text{O}_3$  production yields derived here for the Parish, urban, and coalesced Ship Channel plumes are estimated to be accurate to within a factor of 2. However, the primary conclusion drawn from the large differences observed between plumes from the three different source types (Figure 10a) is more robust. The fractional contribution of  $\text{HNO}_3$  to the products of  $\text{NO}_x$  oxidation in each plume is a function of the ratio of OH to peroxy radicals occurring



during transport. Substantial differences in ( $\text{HNO}_3/(\text{NO}_y - \text{NO}_x)$ ) ratios are apparent in Figure 10b between the Ship Channel and the urban and power plant plumes. The Ship Channel plume was composed of roughly equal amounts of PAN-type compounds and  $\text{HNO}_3$ , while essentially all of the Parish  $\text{NO}_x$  had been oxidized to  $\text{HNO}_3$ , at this distance downwind (Figure 10b) [Neuman *et al.*, 2002]. If  $\text{HNO}_3$  loss had been substantial, accounting for this effect would decrease the  $\text{O}_3$  yields derived from the slope data plotted in Figure 9a. Given the relative amounts of PAN formed, potential losses of  $\text{HNO}_3$  are expected to have been greater in the W.A. Parish plume than for the petrochemical or urban plumes. Any correction to derived  $\text{O}_3$  yields would therefore increase the differences in  $\text{O}_3$  production derived from the plume data in Figure 10a. Similarly, additional  $\text{O}_3$  formation downwind of the northernmost transect is expected to be relatively slow and contribute minimally to derived  $\text{O}_3$  yields, as discussed above. Taking into account observed differences in PAN-type compound abundance relative to total  $\text{NO}_y$ , further  $\text{O}_3$  production would be expected to only increase the differences in yields between these three source types.

#### 4. Discussion

[60] A distinguishing feature of petrochemical plumes is that a substantial amount of reactive hydrocarbons can be coemitted with  $\text{NO}_x$ , in contrast to power plant plumes into which reactive hydrocarbons must be entrained from the surrounding atmosphere. For power plants, then, their location relative to external sources of reactive hydrocarbons is critical in determining the rate and yield of  $\text{O}_3$  formed in plumes downwind [Ryerson *et al.*, 2001]. In contrast, large petrochemical industrial coemission of reactive VOC and  $\text{NO}_x$  is expected to result in appreciable  $\text{O}_3$  formation in the summertime regardless of the geographic location. Despite the hundreds of VOC compounds known to be emitted from petrochemical facilities, VOC measurements aboard the Electra in 2000 suggest that only two alkenes make the largest contribution to prompt  $\text{O}_3$  production in the greater Houston metropolitan area. This finding is not unique to the monthlong Texas 2000 study period. Elevated alkene levels appear to have been characteristic of this area ever since the first measurement campaigns were motivated by passage of the Clean Air Act in 1970, as discussed below.

##### 4.1. Elevated Alkenes in Houston, 1976–2002

[61] Substantially elevated mixing ratios of highly reactive alkenes have been a persistent feature of the Houston area for an extended period of time. Previous studies in the Houston area in 1976 [Gulf Coast Oxidant Study, Decker *et al.*, 1976], 1977 [Houston Area Oxidants Study, HACC, 1979], and in 1993 [Coastal Oxidant Assessment for Southeast Texas, Lawson *et al.*, 1995] and Gulf of Mexico Air Quality Study [Kearney, 1995] have all found very high median mixing ratios of alkenes at sampling sites in the Ship Channel area. These studies suggest that mixing ratios of  $\text{C}_3\text{H}_6$  and  $\text{C}_2\text{H}_4$  in particular have been strongly elevated in the Ship Channel region for over 20 years, beginning with some of the first measurements showing a Houston  $\text{O}_3$  exceedence problem. More recently, 24-hour-integrated

canister VOC samples taken twice a week since 1997 at various locations along the Ship Channel have shown median mixing ratios of  $\text{C}_3\text{H}_6$  (ca. 4 ppbv) and  $\text{C}_2\text{H}_4$  (ca. 12 ppbv) sufficient to dominate VOC reactivity, qualitatively consistent with the findings reported here (W. Crow, personal communication, 2001).

[62] Most recently, on 22 April 2002 the instrumented NOAA WP-3D aircraft sampled the emissions plumes from facilities in Texas City, Chocolate Bayou, Freeport, and Sweeny, as well as that from the Seadrift petrochemical complex near Victoria, TX. Multiple VOC canister samples were acquired in the near-field plume transects (Figure 11) to provide additional data on the (alkene/ $\text{NO}_x$ ) emissions ratios observed during the Texas 2000 study from the Electra aircraft. Measured  $\text{C}_2\text{H}_4$ ,  $\text{C}_3\text{H}_6$ , and  $\text{NO}_x$  are plotted as a function of aircraft longitude to facilitate comparison. In general, while measured (alkene/ $\text{NO}_x$ ) ratios were different than in the same plumes observed in 2000, all were substantially higher than inventories suggest. The Seadrift complex is the largest  $\text{C}_2\text{H}_4$  point source in Texas, according to TNRCC and EPA inventories; however, the measured plume ( $\text{C}_2\text{H}_4/\text{NO}_x$ ) ratio of 4–5 (Figure 10) is still much higher than the annual average emissions ratio of  $\sim 0.5$  derived from these inventories.

#### 5. Conclusions

[63] The principal reactions leading to the rapid  $\text{O}_3$  formation characteristic of the Houston area are shown to involve oxidation of petrochemical emissions of  $\text{C}_3\text{H}_6$  and  $\text{C}_2\text{H}_4$ . This is encouraging for successfully simulating Houston-area petrochemical plume  $\text{O}_3$  production in 3-D atmospheric models that rely on simplified, or lumped, VOC reaction schemes [Dodge, 2000]. The chemical solvers in most 3-D models treat oxidation of the light alkenes explicitly and should be entirely appropriate for modeling prompt  $\text{O}_3$  formation in the Houston area. The principal shortcoming in successful model simulations of prompt  $\text{O}_3$  formation appears to be the substantial underestimate of petrochemical alkene emissions in inventory tabulations. It will be difficult for chemically explicit 3-D models of appropriate spatial resolution to reproduce  $\text{O}_3$  observations in the Houston area until routine petrochemical VOC emissions rates are more realistically included in inventories.

[64] Apparent  $\text{O}_3$  formation rates and yields derived on these 2 days for the isolated complexes and the coalesced Ship Channel plumes are qualitatively similar and are ascribed to similarly elevated (alkene/ $\text{NO}_x$ ) emissions ratios from the aggregated petrochemical facilities at each complex. These rates and yields are substantially higher than those derived on the same day under similar meteorological conditions for the Houston urban plume and that from the W.A. Parish power plant. Further, the urban and power plant yields are qualitatively similar to those reported for other urban areas and rural power plants. Finally, the hourly, daily, and annually averaged emissions suggest that these observations are the result of typical operation of the power plants and petrochemical industrial facilities in the area. Such consistency suggests that the Texas 2000 mission data are representative of the normal effects of various anthropogenic emissions sources on tropospheric  $\text{O}_3$  in the Houston area. We emphasize that while derived values reported



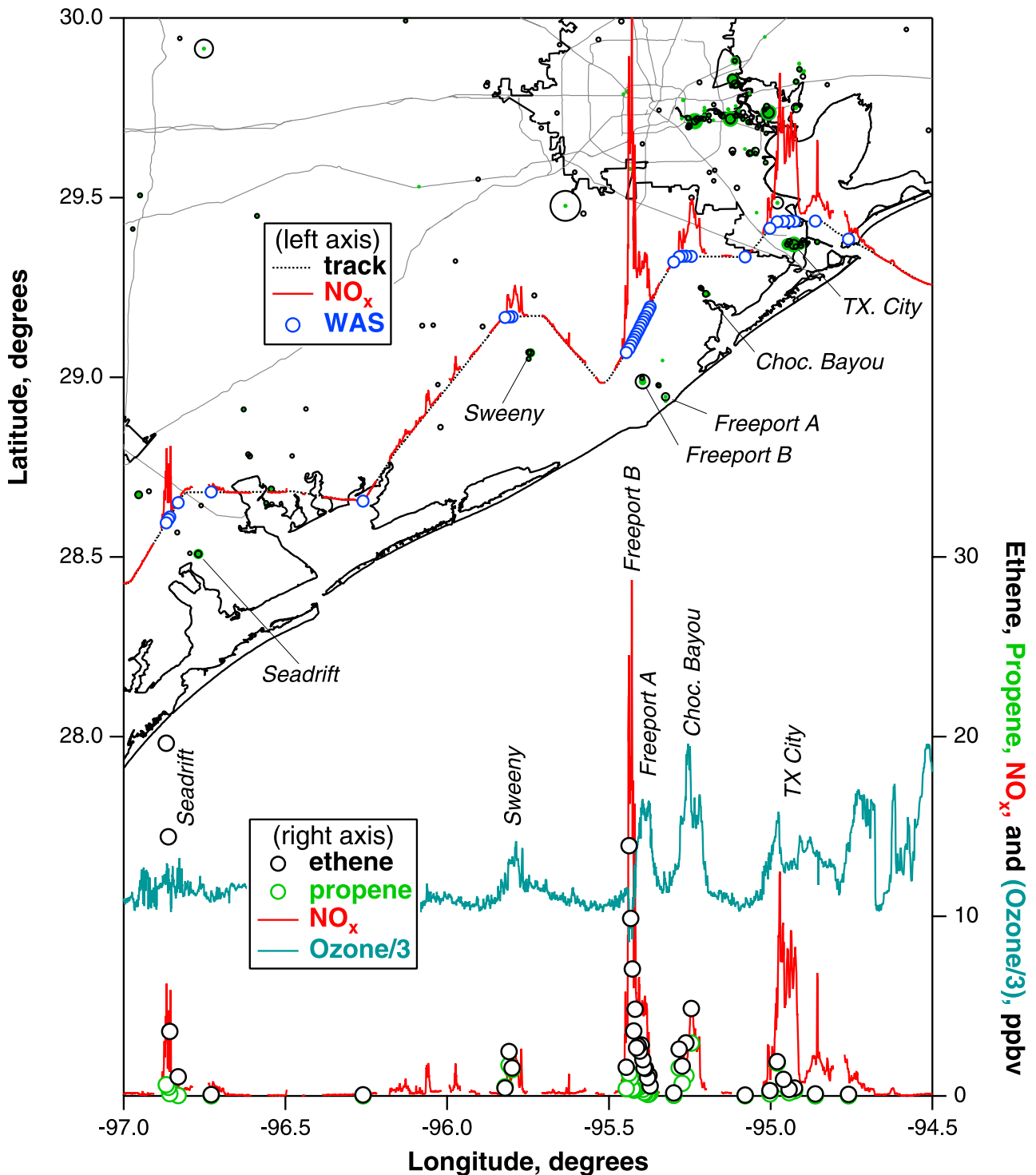


**Figure 11.** A 330 × 250 km map of the Texas Gulf Coast showing measured NO<sub>y</sub> (red line) plotted along the aircraft track at 470 m altitude (dotted line) for the NOAA WP-3D transit flight of 22 April 2002. Blue circles along the track denote sampling locations for the whole-air sample (WAS) volatile organic compound (VOC) canisters. Point sources of NO<sub>x</sub> and VOC are plotted as described in Figure 1; winds were from 150° to 180° for the period shown. Mixing ratios of ethene (heavy black circles), propene (light blue circles), NO<sub>y</sub> (red), and ozone (divided by 3, light blue), are also shown as a function of longitude. Plumes from facilities at Texas City, Chocolate Bayou, Freeport, Sweeny, and the Seadrift petrochemical complex near Victoria, TX, were sampled.

here are subject to substantial day-to-day variability according to meteorological conditions, the differences in O<sub>3</sub> formation rates and yields between the three anthropogenic source types are expected to remain.

[65] The chemistry required to capture the important features of prompt O<sub>3</sub> production in Houston is thus dependent on a limited set of all possible VOCs known to be emitted from petrochemical sources [Derwent, 2000; Watson et al., 2001]. These findings ultimately suggest that correctly estimating emissions of reactive light alkenes should be emphasized in constructing accurate VOC emissions inventories for Houston-area petrochemical industrial sources. Finally, these reactive light alkenes should represent the primary focus of current and future VOC emissions control measures designed to reduce tropospheric O<sub>3</sub> formation from these individual facilities. Reduction in emissions of C<sub>2</sub>H<sub>4</sub> and C<sub>3</sub>H<sub>6</sub> alone would account for over 75% of initial VOC reactivity and by inference the majority of the prompt O<sub>3</sub> formed in the petrochemical plumes studied here. Reductions in emissions of alkanes, other alkenes, and aromatic compounds would be substantially less effective in mitigating rapid O<sub>3</sub> formation in high yield downwind of these sources.

[66] **Acknowledgments.** We thank the staff and flight crew of the NCAR Research Aviation Facility for their support during the Texas 2000 project. Thanks are also due to T. Martin and R. Coulter for providing wind profiler data, to J. Mellberg and J. Neece for compiling the special emissions inventory for the Texas 2000 study, and to J. Meagher for suggestions on the draft manuscript. Participation, suggestions, and cooperation from many companies and individuals from the Houston area petrochemical industry are gratefully acknowledged. This work was funded in part by TNRC and the NOAA Health of the Atmosphere and Climate and Global Change programs.

## References

- Angevine, W. M., A. B. White, and S. K. Avery, Boundary-layer depth and entrainment zone characterization with a boundary-layer profiler, *Boundary Layer Meteorol.*, **68**, 375–385, 1994.
- Atkinson, R., *Gas-Phase Tropospheric Chemistry of Organic Compounds*, Am. Inst. of Phys., Gaithersburg, Md., 1994.
- Atkinson, R., Gas-phase tropospheric chemistry of volatile organic compounds, part I, Alkanes and alkenes, *J. Phys. Chem. Ref. Data*, **26**, 215–290, 1997.
- Banta, R. M., et al., Daytime buildup and nighttime transport of urban ozone in the boundary layer during a stagnation episode, *J. Geophys. Res.*, **103**, 22,519–22,544, 1998.
- Bertman, S. B., J. M. Roberts, D. D. Parrish, M. P. Buhr, P. D. Goldan, W. C. Kuster, F. C. Fehsenfeld, S. A. Montzka, and H. Westberg, Evolution of alkyl nitrates with air mass age, *J. Geophys. Res.*, **100**, 22,805–22,813, 1995.
- Brock, C. A., et al., Particle growth in urban and industrial plumes in Texas, *J. Geophys. Res.*, **108**(D3), 4111, doi:10.1029/2002JD002746, 2003.
- Carter, W. P. L., Development of ozone reactivity scales for volatile organic compounds, *Air Waste*, **44**, 881–899, 1994.
- Chameides, W. L., R. W. Lindsay, J. Richardson, and C. S. Kiang, The role of biogenic hydrocarbons in urban photochemical smog: Atlanta as a case study, *Science*, **241**, 1473–1475, 1988.
- Corbett, J. J., and P. Fischbeck, Emissions from ships, *Science*, **278**, 823–824, 1997.
- Crutzen, P. J., The role of NO and NO<sub>2</sub> in the chemistry of the troposphere and stratosphere, *Annu. Rev. Earth Planet. Sci.*, **7**, 443–472, 1979.
- Daum, P. H., L. Kleinman, D. G. Imre, L. J. Nunnermacker, Y.-N. Lee, S. R. Springston, L. Newman, and J. Weinstein-Lloyd, Analysis of the processing of Nashville urban emissions on July 3 and July 18, 1995, *J. Geophys. Res.*, **105**, 9155–9164, 2000a.
- Daum, P. H., et al., Analysis of O<sub>3</sub> formation during a stagnation episode in central Tennessee in summer 1995, *J. Geophys. Res.*, **105**, 9107–9119, 2000b.
- Davis, D. D., G. Smith, and G. Klauber, Trace gas analysis of power plant plumes via aircraft measurement: O<sub>3</sub>, NO<sub>x</sub>, and SO<sub>2</sub> chemistry, *Science*, **186**, 733–735, 1974.
- Davis, J. M., B. K. Eder, D. Nychka, and Q. Yang, Modeling the effects of meteorology on ozone in Houston using cluster analysis and generalized additive models, *Atmos. Environ.*, **32**, 2505–2520, 1998.
- Decker, C. E., L. A. Ripperton, J. J. B. Worth, F. M. Vukovich, W. D. Bach, J. B. Tommerdahl, F. Smith, and D. E. Wagoner, *Formation and Transport of Oxidants Along Gulf Coast and in Northern U. S.*, Res. Triangle Park, N.C., 1976.
- DeMore, W. B., S. P. Sander, D. M. Golden, R. F. Hampson, M. J. Kurylo, C. J. Howard, A. R. Ravishankara, C. E. Kolb, and M. J. Molina, *Chemical Kinetics and Photochemical Data for Use in Stratospheric Modeling*, NASA Jet Propul. Lab., Pasadena, Calif., 1997.
- Derwent, R. G., Ozone formation downwind of an industrial source of hydrocarbons under European conditions, *Atmos. Environ.*, **34**, 3689–3700, 2000.
- Derwent, R. G., and T. J. Davies, Modelling the impact of NO<sub>x</sub> or hydrocarbon control on photochemical ozone in Europe, *Atmos. Environ.*, **28**, 2039–2052, 1994.
- Dodge, M. C., Chemical oxidant mechanisms for air quality modeling: Critical review, *Atmos. Environ.*, **34**, 2103–2130, 2000.
- EPA, National air quality and emissions trends report, 1999, U.S. Environ. Prot. Agency, Res. Triangle Park, N. C., 2001.
- Flocke, F., A. Volz-Thomas, and D. Kley, Measurements of alkyl nitrates in rural and polluted air masses, *Atmos. Environ., Part A*, **25**, 1951–1960, 1991.
- Fried, A., B. Henry, B. Wert, S. Sewell, and J. R. Drummond, Laboratory, ground-based, and airborne tunable diode laser systems: Performance characteristics and applications in atmospheric studies, *Appl. Phys., Part B*, **67**, 317–330, 1998.
- Gillani, N. V., J. F. Meagher, R. J. Valente, R. E. Imhoff, R. L. Tanner, and M. Luria, Relative production of ozone and nitrates in urban and power plant plumes, 1, Composite results based on data from 10 field measurement days, *J. Geophys. Res.*, **103**, 22,593–22,615, 1998.
- Goldan, P. D., D. D. Parrish, W. C. Kuster, M. Trainer, S. A. McKeen, J. Holloway, B. T. Jobson, D. T. Sueper, and F. C. Fehsenfeld, Airborne measurements of isoprene, CO, and anthropogenic hydrocarbons and their implications, *J. Geophys. Res.*, **105**, 9091–9105, 2000.
- Haagen-Smit, A. J., Chemistry and physiology of Los Angeles smog, *Ind. Eng. Chem.*, **44**, 1342–1346, 1952.
- HACC, Houston Area Oxidants Study program summary, Houston Area Chamber of Commerce, Houston, Tex., 1979.
- Harley, R. A., S. A. McKeen, J. Pearson, M. O. Rodgers, and W. A. Lonnenman, Analysis of motor vehicle emissions during the Nashville/Middle Tennessee Ozone Study, *J. Geophys. Res.*, **106**, 3559–3567, 2001.
- Holloway, J. S., R. O. Jakoubek, D. D. Parrish, C. Gerbig, A. Volz-Thomas, S. Schmitgen, A. Fried, B. Wert, B. Henry, and J. R. Drummond, Airborne intercomparison of vacuum ultraviolet fluorescence and tunable diode laser absorption measurements of tropospheric carbon monoxide, *J. Geophys. Res.*, **105**, 24,251–24,261, 2000.
- Kalabokas, P. D., J. Hatzianestis, J. G. Bartzis, and P. Papagiannakopoulos, Atmospheric concentrations of saturated and aromatic hydrocarbons around a Greek oil refinery, *Atmos. Environ.*, **35**, 2545–2555, 2001.
- Kearney, A. T., Gulf of Mexico air quality study, final report, vol. I, summary of data analysis and modeling, U.S. Dep. of Inter., New Orleans, La., 1995.
- Kleinman, L., P. H. Daum, D. G. Imre, C. Cardelino, K. J. Olszyna, and R. G. Zika, Trace gas concentrations and emissions in downtown Nashville during the 1995 Southern Oxidants Study/Nashville Intensive, *J. Geophys. Res.*, **103**, 22,545–22,553, 1998.
- Kleinman, L. I., P. H. Daum, D. G. Imre, J. H. Lee, Y.-N. Lee, L. J. Nunnermacker, S. R. Springston, J. Weinstein-Lloyd, and L. Newman, Ozone production in the New York City urban plume, *J. Geophys. Res.*, **105**, 14,495–14,512, 2000.
- Kleinman, L. I., P. H. Daum, D. G. Imre, Y.-N. Lee, L. J. Nunnermacker, S. R. Springston, J. Weinstein-Lloyd, and J. Rudolph, Ozone production rate and hydrocarbon reactivity in 5 urban areas: A cause of high ozone concentration in Houston, *Geophys. Res. Lett.*, **29**, 10.1029/2001GL014569, 2002.
- Lawson, D. R., N. F. Robinson, S. Diaz, J. G. Watson, E. M. Fujita, and P. T. Roberts, Coastal oxidant assessment for southeast Texas (COAST) project: Final report, Desert Res. Inst., Reno, Nev., 1995.
- Leighton, P. A., *Photochemistry of Air Pollution*, 300 pp., Academic, San Diego, Calif., 1961.
- Levy, H., Normal atmosphere: Large radical and formaldehyde concentrations predicted, *Science*, **173**, 141–143, 1971.
- Liu, S. C., M. Trainer, F. C. Fehsenfeld, D. D. Parrish, E. J. Williams, D. W. Fahey, G. Hübler, and P. C. Murphy, Ozone production in the rural troposphere and the implications for regional and global ozone distributions, *J. Geophys. Res.*, **92**, 4191–4207, 1987.
- Luria, M., R. J. Valente, R. L. Tanner, N. V. Gillani, R. E. Imhoff, S. F. Mueller, K. J. Olszyna, and J. F. Meagher, The evolution of photoche-

- mical smog in a power plant plume, *Atmos. Environ.*, **33**, 3023–3026, 1999.
- Luria, M., R. L. Tanner, R. E. Imhoff, R. J. Valente, E. M. Bailey, and S. F. Mueller, Influence of natural hydrocarbons on ozone formation in an isolated power plant plume, *J. Geophys. Res.*, **105**, 9177–9188, 2000.
- Miller, D. F., A. J. Alkezweeny, J. M. Hales, and R. N. Lee, Ozone formation related to power plant emissions, *Science*, **202**, 1186–1188, 1978.
- Neuman, J. A., et al., Fast-response airborne in situ measurements of HNO<sub>3</sub> during the Texas 2000 Air Quality Study, *J. Geophys. Res.*, **107**(D20), 4436, doi:10.1029/2001JD001437, 2002.
- Nicks, D. K., Jr., et al., Fossil-fueled power plants as a source of atmospheric carbon monoxide, *J. Environ. Monit.*, **5**, 35–39, 2003.
- Nunnermacker, L. J., L. I. Kleinman, D. Imre, P. H. Daum, Y.-N. Lee, J. H. Lee, S. R. Springston, L. Newman, and N. Gillani, NO<sub>y</sub> lifetimes and O<sub>3</sub> production efficiencies in urban and power plant plumes: Analysis of field data, *J. Geophys. Res.*, **105**, 9165–9176, 2000.
- Parrish, D. D., M. Trainer, M. P. Buhr, R. Watkins, and F. C. Fehsenfeld, Carbon monoxide concentrations and their relation to concentrations of total reactive oxidized nitrogen at two rural U.S. sites, *J. Geophys. Res.*, **96**, 9309–9320, 1991.
- Parrish, D. D., M. Trainer, D. Hereid, E. J. Williams, K. J. Olszyna, R. A. Harley, J. F. Meagher, and F. C. Fehsenfeld, Decadal change in carbon monoxide to nitrogen oxide ratio in U.S. vehicular emissions, *J. Geophys. Res.*, **107**(D12), 4140, doi:10.1029/2001JD000720, 2002.
- Placet, M., C. O. Mann, R. O. Gilbert, and M. J. Niefer, Emissions of ozone precursors from stationary sources: A critical review, *Atmos. Environ.*, **34**, 2183–2204, 2000.
- Ridley, B. A., E. L. Atlas, J. G. Walega, G. L. Kok, T. A. Staffelbach, J. P. Greenberg, F. E. Grahek, P. G. Hess, and D. D. Montzka, Aircraft measurements made during the spring maximum of ozone over Hawaii: Peroxides, CO, O<sub>3</sub>, NO<sub>3</sub>, condensation nuclei, selected hydrocarbons, halocarbons, and alkyl nitrates between 0.5 and 9 km altitude, *J. Geophys. Res.*, **102**, 18,935–18,961, 1997.
- Ryerson, T. B., et al., Emissions lifetimes and ozone formation in power plant plumes, *J. Geophys. Res.*, **103**, 22,569–22,583, 1998.
- Ryerson, T. B., L. G. Huey, K. Knapp, J. A. Neuman, D. D. Parrish, D. T. Sueper, and F. C. Fehsenfeld, Design and initial characterization of an inlet for gas-phase NO<sub>y</sub> measurements from aircraft, *J. Geophys. Res.*, **104**, 5483–5492, 1999.
- Ryerson, T. B., E. J. Williams, and F. C. Fehsenfeld, An efficient photolysis system for fast-response NO<sub>2</sub> measurements, *J. Geophys. Res.*, **105**, 26,447–26,461, 2000.
- Ryerson, T. B., et al., Observations of ozone formation in power plant plumes and implications for ozone control strategies, *Science*, **292**, 719–723, 2001.
- Schauffler, S., E. L. Atlas, D. R. Blake, F. Flocke, R. A. Lueb, J. M. Lee-Taylor, V. Stroud, and W. Trivicek, Distributions of brominated organic compounds in the troposphere and lower stratosphere, *J. Geophys. Res.*, **104**, 21,513–21,535, 1999.
- Senff, C. J., R. M. Hardesty, R. J. I. Alvarez, and S. D. Mayor, Airborne lidar characterization of power plant plumes during the 1995 Southern Oxidants Study, *J. Geophys. Res.*, **103**, 31,173–31,189, 1998.
- Sexton, K., and H. Westberg, Ambient air measurements of petroleum refinery emissions, *J. Air Pollut. Control Assoc.*, **29**, 1149–1152, 1979.
- Sexton, K., and H. Westberg, Photochemical ozone formation from petroleum refinery emissions, *Atmos. Environ.*, **17**, 467–475, 1983.
- Sillman, S., Ozone production efficiency and loss of NO<sub>x</sub> in power plant plumes: Photochemical model and interpretation of measurements in Tennessee, *J. Geophys. Res.*, **105**, 9189–9202, 2000.
- Stutz, J., and U. Platt, Improving long-path differential optical absorption spectroscopy with a quartz-fiber mode mixer, *Appl. Opt.*, **36**, 1105–1115, 1997.
- Trainer, M., E.-Y. Hsie, S. A. McKeen, R. Tallamraju, D. D. Parrish, F. C. Fehsenfeld, and S. C. Liu, Impact of natural hydrocarbons on hydroxyl and peroxy radicals at a remote site, *J. Geophys. Res.*, **92**, 11,879–11,894, 1987a.
- Trainer, M., E. J. Williams, D. D. Parrish, M. P. Buhr, E. J. Allwine, H. H. Westberg, F. C. Fehsenfeld, and S. C. Liu, Models and observations of the impact of natural hydrocarbons on rural ozone, *Nature*, **329**, 705–707, 1987b.
- Trainer, M., et al., Correlation of ozone with NO<sub>y</sub> in photochemically aged air, *J. Geophys. Res.*, **98**, 2917–2925, 1993.
- Trainer, M., B. A. Ridley, M. P. Buhr, G. Kok, J. Walega, G. Hübler, D. D. Parrish, and F. C. Fehsenfeld, Regional ozone and urban plumes in the southeastern United States: Birmingham, a case study, *J. Geophys. Res.*, **100**, 18,823–18,834, 1995.
- Watson, J. G., J. C. Chow, and E. M. Fujita, Review of volatile organic compound source apportionment by chemical mass balance, *Atmos. Environ.*, **35**, 1567–1584, 2001.
- Wert, B. P., et al., Signatures of terminal alkene oxidation in airborne formaldehyde measurements during TexAQS 2000, *J. Geophys. Res.*, **108**(D3), 4104, doi:10.1029/2002JD002502, 2003.
- White, W. H., J. A. Anderson, D. L. Blumenthal, R. B. Husar, N. V. Gillani, J. D. Husar, and W. E. J. Wilson, Formation and transport of secondary air pollutants: Ozone and aerosols in the St. Louis urban plume, *Science*, **194**, 187–189, 1976.
- Wiedinmyer, C., A. Guenther, M. Estes, I. W. Strange, G. Yarwood, and D. T. Allen, A land-use database and examples of biogenic isoprene emission estimates for the state of Texas, USA, *Atmos. Environ.*, **35**, 6465–6477, 2001.
- Winner, D. A., and G. R. Cass, Modeling the long-term frequency distribution of regional ozone concentrations, *Atmos. Environ.*, **33**, 431–461, 1999.

R. J. Alvarez, R. M. Banta, L. S. Darby, and C. J. Senff, Environmental Technology Laboratory, National Oceanic and Atmospheric Administration, 325 Broadway, Boulder, CO 80305, USA.

W. M. Angevine, C. A. Brock, F. C. Fehsenfeld, G. J. Frost, P. D. Goldan, J. S. Holloway, G. Hübler, R. O. Jakoubek, W. C. Kuster, J. A. Neuman, D. K. Nicks Jr., D. D. Parrish, J. M. Roberts, T. B. Ryerson, D. T. Sueper, and M. Trainer, Aeronomy Laboratory, National Oceanic and Atmospheric Administration, R/E/AL7, 325 Broadway, Building 22, Boulder, CO 80303, USA. (tryerson@al.noaa.gov)

E. L. Atlas, S. G. Donnelly, F. Flocke, A. Fried, W. T. Potter, S. Schauffler, V. Stroud, A. J. Weinheimer, B. P. Wert, and C. Wiedinmyer, Atmospheric Chemistry Division, National Center for Atmospheric Research, P. O. Box 3000, Boulder, CO 80307, USA.

R. W. Dissly, Ball Aerospace Corporation, 1600 Commerce Street, Boulder, CO 80301, USA.